Study of thermosensitive heterogeneous media via space-time homogenization

Claude Boutin, Henri Wong

Study of thermosensitive heterogeneous media via space–time homogenisation

Claude Boutin, Henri Wong *

Laboratoire Géomatériaux, Département Génie Civil et Bâtiment (CNRS URA 1652),
École Nationale des Travaux Publics de l'État, rue Maurice Audin, 69518 Vaulx-en-Velin cedex, France

Abstract – In this paper is presented a theoretical study on the coupled thermosensitive behaviour of heterogeneous, biphasic materials subjected to harmonic excitations of long duration (fatigue tests for example), by a double homogenisation approach — with respect to both space and time. Applied to the thermal problem, this results in the differentiation of several qualitatively different evolutions in the temperature field. For the mechanical aspect, heat generated by mechanical work leads to temperature rises, which in turn reduce the material moduli, resulting in a bilateral coupling. It is shown that this effect is significant in the case of bituminous concrete. The evolution of the material properties takes place, however, generally on a much longer time-scale than the period of excitation. A double homogenisation approach then results in an entirely macroscopic description.

thermosensitive behaviour / space–time homogenisation / heterogeneous media / thermal viscoelasticity / bilateral thermomechanical couplings / complex compliance tensor / asymptotic analysis / multiple-scale variables

1. Introduction

In this paper, we study the macroscopic (with respect to a pertinent scale of observation) behaviour of temperature-sensitive biphasic composite materials subjected to a large number of cyclic loadings, starting from the rheological behaviour of each phase on a local scale. Common examples are fatigue load tests of bituminous concrete or resinous concrete. Besides the classic double space-scales in the study of heterogeneous media, the present problem also involves two distinct time-scales. Indeed, the *rapidly* oscillating load, which defines a microchronological time-scale, generates heat *slowly* through the mechanical work done, which in turn modifies *progressively* the mechanical properties. The method of homogenisation of periodical structures is applied simultaneously with respect to space and time to treat these aspects.

Note that our objective here is to obtain macroscopic descriptions useful for practical applications by formal asymptotic analyses. Aspects related to mathematical convergence are not treated in this paper.

The work presented here differs from previous macroscopic thermomechanical descriptions of heterogeneous media for example those found in Sanchez Palencia (1980) and Francfort and Suquet (1986). In these papers, the mechanical behaviour is temperature-independent; coupling arises from thermal dilation, due to heat generated by mechanical dissipation. This coupling was further suppressed in Francfort and Suquet (1986) by setting a null thermal expansivity, in order to establish convergence results. In this paper, thermal expansion is also neglected. However, coupling due to thermosensitivity of the material — mechanical dissipation generates heat, which in turn modifies the material properties and changes the dissipative power — is accounted for.

* Correspondence and reprints

After a brief review of the governing constitutive equations in each of the two phases — an elastic solid skeleton filled by a viscoelastic thermosensitive medium — and the principle of the homogenisation method, based on asymptotic analysis and use of multiple-scale variables, the mechanical problem under isothermal conditions is first reviewed. When scale separation is possible, which is explicitly assumed here, space homogenisation leads to the constitutive equations of an equivalent, macroscopically homogeneous material, and at the same time the mascroscopic rheological parameters, such as the complex stiffness tensor and the average mechanical dissipation. In the absence of temperature variation, there are, however, no slow-varying quantities, and the adequate time-scale only depends on the loading frequency.

The problem of thermal diffusion in a heterogeneous medium, with an arbitrary time-dependent distributed source, is then considered. The space–time homogenisation approach shows that four qualitatively different situations are possible, depending on the relative magnitudes of the conductive, inertial and source terms. For each particular combination of material constants and source intensity, the analysis shows whether macroscopic descriptions — either space or time, or both — are available. The conclusions have a general character, and are applicable independently of the mechanical problem.

The combined thermomechanical problem, taking into account simultaneously the heat generated due to mechanical dissipation and the material softening due to heating, is then formulated in the light of the preceding analyses. The thermal power due to mechanical dissipation being identified, the thermal diffusion problem is completely defined, giving a macroscopic solution under specified conditions. Finally, substitution of the temperature field in the mechanical problem allows one to obtain the macrochronological drift of the macroscopic quantities.

The final result is a system of coupled, partial differential equations, which together with the initial and boundary conditions, defines a classic boundary value problem. Its numerical solution is straight forward and necessitates the same amount of computations as in the case of a homogeneous material with a slowly varying load/heat source.

An idealised case of a multi-layered medium, which has a semi-analytical solution, is treated in detail, in order to illustrate the main concepts developed.

2. General assumptions

2.1. Geometry, loading and quasi-static behaviour

We are interested in the thermosensitive behaviour of a heterogeneous body occupying a volume V in a three-dimensional space (*figure 1*). This body is supposed to be composed of two distinct materials — one linear elastic and the other viscoelastic and thermosensitive, both of which are homogeneous and isotropic — referred to hereafter as the elastic phase and the viscoelastic phase. On a local scale, the thermomechanical properties are supposed to be perfectly periodical, made up of identical unit cells Ω (*figure 1*), while each unit cell Ω can be partitioned into Ω_s ('s' for the elastic phase) and Ω_f ('f' for the viscoelastic phase). We shall denote by $|\Omega|$ the volume of Ω, and n the volume fraction of the viscoelastic phase

$$n = \frac{|\Omega_f|}{|\Omega|} < 1 \tag{1}$$

Only small displacements and small strains are considered here. Attention will be concentrated on quasi-static behaviour under harmonic excitations. In the absence of body forces, the general equation of motion $\mathrm{div}(\sigma) + F = \rho\ddot{U}$ reduces to the following equation of static equilibrium

$$\mathrm{div}(\sigma) = 0 \tag{2}$$

a.

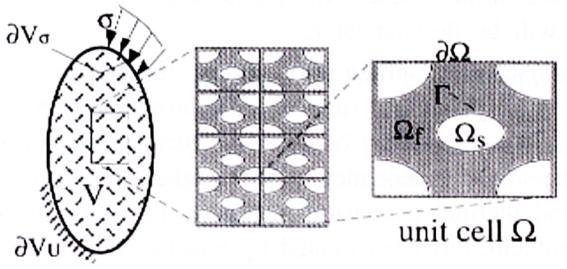

b.

Figure 1. Example of a biphasic material (**a**) and its geometric idealisation (**b**);
(**a**) a typical bituminous concrete sample in fatigue tests; (**b**), geometry of the heterogeneous periodical biphasic medium under study.

Despite the linear constitutive law (to be introduced in Section 2.2) and the non-consideration of inertial forces, mechanical dissipation coupled with thermosensitivity introduce non-linearities, and the material responses (displacements and strains) are in general not harmonic. Nonetheless, limiting ourselves at the moment to situations where such non-linearities are 'small' (small dissipative power, therefore slow evolution of material constants), for short durations (in the order of the excitation period $t_e = 2\pi/\omega$), the structural response is quasi-harmonic, and may be represented by the real part of a complex function of the form

$$U = \mathbb{U}e^{i\omega t} \tag{3}$$

where $\mathbb{U}$ may be complex or real, and varies on a time-scale that is much longer than the excitation period. The notation $||.||$ will be used to denote the amplitude of a complex number, for example: $||e^{i\omega t}|| = 1$. No particular notation will be used to distinguish scalars from tensors; the context should make their distinction unambiguous. The limit of validity of the quasi-harmonic response (3) will be reviewed in Section 7.

2.2. *Mechanical behaviour of constituents*

2.2.1. *Elastic phase*

Not taking thermal dilation into account, the constitutive relation of the elastic phase is written

$$\sigma^s = a : e(U_s) \quad (\text{i.e. } \sigma^s_{ij} = a_{ijkl}e_{kl}(U_s)) \tag{4}$$

where $e(U) = \frac{1}{2}(\nabla U + {}^t\nabla U)$ is the linearised strain tensor, and a_{ijkl} the classic elastic moduli, supposed to be temperature-independent, and ':' represents a double contraction between two tensors. Linearity of the operator e implies that the strain rate tensor d is given by

$$d(\dot{U}) = e(i\omega U) = i\omega e(U) \tag{5}$$

2.2.2. Viscoelastic thermosensitive phase

The behaviour of the viscoelastic thermosensitive phase, under the hypotheses of uncompressibility and harmonic excitations, is described by Eqs (6) and (7) below

$$\sigma^f = -P1 + 2M^*(\omega, \theta)e(U_f) \tag{6}$$

$$\mathrm{div}(U_f) = 0 \tag{7}$$

where $P = -\mathrm{Tr}(\sigma^f)$ is the mean pressure, M^* the complex modulus — *a function of temperature* θ and angular frequency ω — and div the divergence operator. Equation (7) implies that $e(U_f)$ is a pure deviator with $\mathrm{Tr}(e(U_f)) = 0$. The viscous behaviour introduces a positive mechanical dissipation and leads to temperature rises. The increase in temperature in turn reduces the modulus M^* and softens the material. The precise form of the mechanical dissipation will be derived later.

The thermosensitivity of the viscoelastic phase is of central importance in our analysis. To fix ideas, in the case of bitumen, a 1 °C rise in temperature results in an approximately 5 % drop in the amplitude of M^*. This factor introduces a truly bilateral coupling between the mechanical and the thermal problems, in such a way that no one problem can be solved independently of the other. The case where the mechanical parameters are temperature-independent and thermal expansion negligible ($\alpha = 0$), so that the mechanical problem is decoupled from the thermal problem, has been treated by Sanchez Palencia (1980) and Francfort and Suquet (1986) with a convergence result.

2.3. Thermal behaviour of constituents

Both elastic and viscoelastic phases are supposed to obey the classic Fourier's law of thermal conduction, where the heat flux q is related to the thermal gradient by $q = -\lambda\nabla\theta$, and the temperature field verifies the classic heat equation

$$(\rho C)^\mu \dot{\theta}^\mu - \mathrm{div}[\lambda_\mu \nabla\theta^\mu] = S_\mu \tag{8}$$

(ρC) is the specific heat per unit volume and λ the thermal conductivity — both supposed to be constant. S is the internal heat source due to mechanical dissipation, to be derived here below. Here μ is to be replaced by 's' in the elastic phase and by 'f' in the viscoelastic phase.

2.3.1. Heat source in the elastic phase

The only heat source considered comes from the coupling effect. For the elastic phase, the instantaneous source S_s takes the following form (see e.g. Fung, 1968)

$$S_s = -\theta^s a_{ijkl}\alpha^s_{ij} d_{kl} \tag{9}$$

where α^s_{ij} are the thermal dilation coefficients of the elastic phase, while θ^s is the absolute temperature. When the displacement is a harmonic function of time, S_s represents small fluctuations around a zero average value, and its long-term effects are negligible. If we further do not take into account thermal dilations ($\alpha^s_{ij} = 0$), then S_s is identically zero. This last assumption, adopted in the rest of this paper, is partly justified by the small

temperature changes (a few degrees) and the amplitude of the coefficients α_{ij}^s (in the order of $10^{-6}/°C$, and partly by the prevailing 'unconfined' conditions for the problems considered.

2.3.2. Heat source in the viscoelastic thermosensitive phase

As for the elastic phase, we suppose that $\alpha_{ij}^f = 0$. However, non-zero mechanical dissipation intervenes in the viscoelastic phase. For the constitutive law (6) and at a fixed excitation frequency ω, the material behaviour can be ascribed to the Kelvin–Voigt type. Hence, we may write the stress as the sum of a reversible and an irreversible component

$$\sigma^f = \sigma_r^f + \sigma_{ir}^f \tag{10}$$

$$\sigma_r^f = -P1 + 2M_r e(U_f); \quad \sigma_{ir}^f = \frac{2M_i}{\omega} d(\dot{U}_f) \tag{11}$$

The mechanical dissipation is given by $Re\{\sigma_{ir}^f\} : Re\{d(\dot{U}_f)\}$. Putting $U_f = u_f e^{i(\phi+\omega t)}$, where $u_f = ||U_f||$ and ϕ is the phase-lag, the last expression simplifies to

$$S_f = 2\omega M_i \sin^2(\omega t + \phi) e(u_f) : e(u_f) \tag{12}$$

3. Thermosensitive behaviour of a biphasic medium subject to harmonic loading: general setting

We are interested in the simultaneous evolution of the fully coupled displacement and temperature fields inside the heterogeneous body V. The knowledge of the displacement field leads to the deduction of the strain and stress fields through the constitutive relations.

3.1. Mechanical problem

In the elastic phase, eliminating σ^s from the equilibrium and constitutive equations (2) and (4) leads to

$$\mathrm{div}[a : e(U_s)] = 0 \quad \text{in } \Omega_s \tag{13}$$

while a similar operation for the viscoelastic phase gives

$$\mathrm{div}[-P1 + 2M^*(\omega, \theta) e(U_f)] = 0 \quad \text{in } \Omega_f \tag{14}$$

bearing in mind the uncompressibility condition

$$\mathrm{div}(U_f) = 0 \quad \text{in } \Omega_f \tag{15}$$

The displacement and the stress vectors are continuous across the phase boundary Γ (*figure 1*), thus

$$a : e(U_s) \cdot N = [-P1 + 2M^*(\omega, \theta) e(U_f)] \cdot N \quad \text{on } \Gamma \tag{16}$$

$$U_s = U_f \quad \text{on } \Gamma \tag{17}$$

At the boundary of the body V, either displacement or surface tractions are specified

$$U_\mu = U^d \quad \text{on } \partial V_u \tag{18}$$

$$\sigma^\mu \cdot N = T^d \quad \text{on } \partial V_\sigma \tag{19}$$

$U^d(x,t)$ and $T^d(x,t)$ respresents the imposed boundary displacements and stresses, of the form

$$U^d = ||U^d|| e^{i\omega t}; \quad T^d = ||T^d|| e^{i\omega t} \tag{20}$$

Equations (13)–(20) define the mechanical problem of the composite body V, where the notation $M^*(\omega, \theta)$ highlights the coupling with temperature. As mentioned in Section 2.1, we will seek a solution of the form

$$U_\mu = \mathcal{U}_\mu e^{i\omega t} \tag{21}$$

3.2. Thermal problem

The heat equation must be satisfied at every point within the body V

$$(\rho C)^\mu \dot{\theta}^\mu - \operatorname{div}[\lambda_\mu \nabla \theta^\mu] = S_\mu \tag{22}$$

where

$$S_s = 0 \quad \text{in } \Omega_s \tag{23}$$

$$S_f = 2\omega M_i \sin^2(\omega t + \phi)\, e(u_f) : e(u_f) \quad \text{in } \Omega_f \tag{24}$$

At the interface Γ, both temperature and the normal heat flux are continuous

$$\theta^s = \theta^f \quad \text{on } \Gamma \tag{25}$$

$$\lambda_s \nabla \theta^s \cdot N = \lambda_f \nabla \theta^f \cdot N \quad \text{on } \Gamma \tag{26}$$

while on the macroscopic boundary, either the temperature or the heat flux are specified

$$\theta^\mu = \theta^d(x) \quad \text{on } \partial V_\theta \tag{27}$$

$$-\lambda_\mu \nabla \theta^\mu \cdot N = q^d(x) \quad \text{on } \partial V_q \tag{28}$$

Equations (22)–(28) define the thermal problem. Coupling with the mechanical problem arises through the heat source S_f in (24) which depends explicitly on the displacement field u_f.

Hence thermomechanical coupling intervenes in both directions: mechanical dissipation S_f generates heat while inversely, the heat generated softens the materials and modifies the dissipative power. In consequence, both the displacement amplitude $||U_\mu||$ and the phase-lag in (21) will vary with time, whereas they would have remained constant had the material behaviour been temperature-independent.

In addition, the microstructure and the cyclic loading generate fast-varying local fluctuations, with respect to both space and time. Nonetheless, it is rather the long-term 'drifts', such as strain and stress amplitude variations, or global rise in temperatures, which are of practical interest. This justifies our research into such long-term drifts by the method of homogenisation.

3.3. Principle of the homogenisation method

3.3.1. Space homogenisation

The aim of spatial homogenisation is to obtain a 'continuum' description at the macroscopic level, starting from the descriptions of the microstructural components.

Obviously, it is impossible to obtain a macroscopic description if the underlying phenomenon varies essentially at the level of local heterogeneities. An essential condition to be satisfied is that the phenomenon presents a characteristic length of variation L (within a body of comparable or larger size), much larger than that of the local heterogeneities l. Hence, the search for a homogenised behaviour makes sense only if the condition of *scale separation* is fulfilled. Actually, this condition leads to two requirements which result in a 'local invariance': a) the first concerns the material: it must be sufficiently regular so that one can define a (elementary) *representative*

volume element (RVE) of a characteristic microscopic size l; b) the second is related to the phenomenon in question: the characteristic length L of its variations must be large in comparison with l.

If these two conditions are fulfilled, a macroscopic variation in the phenomenon over the microstructures can be discerned, and the problem can be treated using standard continuum mechanics. The space homogenisation of periodic structures uses asymptotic and multiple-scale analyses (Sanchez–Palencia, 1980). The two well-distinct space-scales lead to the use of two space-variables, x and y: x describes variations on the macroscopic scale, and y describes variations on the microstructural scale. The small parameter ε_1 ($\varepsilon_1 \ll 1$) denotes the space-scale ratio

$$\varepsilon_1 = l/L \qquad x = \varepsilon_1 y$$

For a given problem, the value of ε_1 can be assessed by estimating L using a dimensional analysis on the macroscopic scale (Boutin and Auriault, 1990).

Use of the double space variables transforms the common spatial derivatives at the macroscopic (respectively microscopic) space-scale into $\partial_x + \varepsilon_1^{-1}\partial_y$ (respectively $\partial_y + \varepsilon_1 \partial_x$). Due to the different orders of magnitude introduced by ε_1, the variables are expressed in the form of asymptotic expansions in powers of ε_1. For example, with respect to the displacement U, we have

$$U(x,y) = U^0(x,y) + \varepsilon_1^1 U^1(x,y) + \varepsilon_1^2 U^2(x,y) + \ldots \quad \text{with:} \quad O(U^k/U^0) = 1 \qquad (29)$$

while the usual differential operations on the macroscopic scale on U will be modified. Using the suffix 'x' or 'y' to indicate the independent space variable with respect to which derivatives are taken, we have for example

$$\begin{aligned} \mathrm{div}[a : e(U)] = {} & \varepsilon_1^{-2}\mathrm{div}_y[a : e_y(U^0)] + \varepsilon_l^{-1}\{\mathrm{div}_x[a : e_y(U^0)] + \mathrm{div}_y[a : (e_x(U^0) + e_y(U^1))]\} \\ & + \varepsilon_1^0\{\mathrm{div}_x[a : (e_x(U^0) + e_y(U^1))] + \mathrm{div}_y[a : (e_x(U^1) + e_y(U^2))]\} + \cdots \end{aligned} \qquad (30)$$

A specificity of this method is to express the existence of a RVE through the assumption of the *periodicity of the microstructure*. This microstructural periodicity induces an identical periodicity on the functions U^k, with respect to the local coordinate y.

The process consists of introducing the series representation (29) in the equations governing the physics, then identifying the terms of the same power in ε_1, and finally solving recursively the problems obtained for each power.

In principle, this method is all the more precise as ε_1 is small compared to 1, that is, when the two scales are clearly distinguished. In this case, the description obtained *at the first significant order* defines the equivalent continuum behaviour of the material, with an accuracy of $O(\varepsilon_1)$.

3.3.2. Time homogenisation

In a similar manner, some phenomena may exhibit fast-varying, quasi-periodic temporal fluctuations, but show a remarkably smooth and gradual progression when examined over a long duration of time. The temperature rise in a bituminous concrete sample during a fatigue test is a good illustration of this double-scale temporal evolution: the rapid temperature fluctuations on a microchronological scale are governed by the period t_e ($t_e = 2\pi/\omega$) of the cyclic load, while a progressive temperature rise on a longer time-scale can be discerned.

In this latter case, the condition of scale separation depends on the duration of observation $\tilde{t}$. When $\tilde{t}/t_e \gg 1$, scale separation is possible, and a macrochronological description, focussed on the 'slow', progressive variations (analogue to the macroscopic description above), can be found.

As in space homogenisation, we will define two time-scales: a microchronological time-scale with t_e as the reference duration, and a macrochronological time-scale with a much longer reference duration $\tilde{t}$, such that a second small parameter ε_t ($\varepsilon_t \ll 1$, in general different from ε_1) denotes the time-scale ratio

$$\varepsilon_t = \frac{t_e}{\tilde{t}}$$

We will denote the corresponding 'micro' and 'macro' time coordinates by t and T, such that

$$T = \varepsilon_t t$$

An example of time homogenisation can be found in Guennouni (1988). An analysis simultaneously using space and time homogenisation can for example be found in Dormieux et al. (1993).

In the following section, we will begin by considering the particular case when temperature changes are negligible, hence the rheological parameters remain constant. In consequence, there are no slow-varying (with time) quantities, and only one time-scale — the one imposed by the cyclic loading — is pertinent.

4. Space homogenisation of the mechanical problem under isothermal conditions

The following presentation follows the same line of reasoning as in Boutin and Auriault (1990), where the same method of formal asymptotics was used. Since there is only one small parameter ε_1, related to the double space-scales, we will simply write ε instead of ε_1 to simplify.

4.1. Main assumptions

We shall assume that i) temperatures remain at the reference value θ_{ref} everywhere. Hence, all rheological parameters remain constant; ii) a macroscopic space-scale exists, such that $l/L \ll 1$; iii) the displacement field is harmonic (i.e. $\dot{U} = i\omega U$); iv) the viscoelastic stresses and the elastic stresses are of the same order of magnitude. Inertial and gravity forces are not taken into account.

4.2. Space homogenisation

From i), $M^* = M^*_{ref} = M^*(\omega, \theta_{ref})$ remains constant. With assumption iv), the system of equations (13)–(20) written in macroscopic coordinates and local time coordinates need not be renormalised. Taking terms of the order ε^{-2} in (13), ε^{-2} in (14), ε^{-1} in (16), ε^0 in (17) and ε^{-1} in (15), the following homogeneous system of linear equations is obtained (Boutin and Auriault, 1990)

$$\begin{aligned}
&\mathrm{div}_y[a : e_y(U_s^0)] = 0 && \text{in } \Omega_s \\
&\mathrm{div}_y[M^*_{ref} e_y(U_f^0)] = 0 && \text{in } \Omega_f \\
&a : e_y(U_s^0) \cdot N = 2M^*_{ref} e_y(U_f^0) \cdot N && \text{on } \Gamma \\
&U_s^0 = U_f^0 && \text{on } \Gamma \\
&\mathrm{div}_y(U_f^0) = 0 && \text{in } \Omega_f
\end{aligned} \tag{31}$$

which leads to the conclusion that $U_s^0 = U_f^0 = U^0(x,t)$ is independent of y. Terms of an order higher give

$$\begin{aligned}
&\mathrm{div}_y[a : \{e_x(U^0) + e_y(U_s^1)\}] = 0 && \text{in } \Omega_s \\
&-\nabla_y P^0 + 2\mathrm{div}_y[M_{ref}^*(e_x(U^0) + e_y(U_f^1))] = 0 && \text{in } \Omega_f \\
&a : \{e_x(U^0) + e_y(U_s^1)\} \cdot N = \{-P^0 1 + 2M_{ref}^*[e_x(U^0) + e_y(U_f^1)]\} \cdot N && \text{on } \Gamma \\
&U_s^1 = U_f^1 && \text{on } \Gamma \\
&\mathrm{div}_x(U^0) + \mathrm{div}_y(U_f^1) = 0 && \text{in } \Omega_f
\end{aligned} \tag{32}$$

It is evident that U_s^1, U_f^1 and P^0 depend linearly on $e_x(U^0)$. Noting that $U^1 = U_s^1$ in Ω_s and $U^1 = U_f^1$ in Ω_f, we can write

$$U^1 = U^1(x,t) + \chi_{ref}^{\alpha\beta}(y) e_{x\alpha\beta}(U^0) \tag{33}$$

$$P^0 = P^1(x,t) - \tau_{ref}^{\alpha\beta}(y) e_{x\alpha\beta}(U^0) \tag{34}$$

Here, the vector fields $\chi_{ref}^{\alpha\beta}(y)$ and the scalar fields $\tau_{ref}^{\alpha\beta}(y)$, defined up to an arbitrary constant, are the particular solutions of problem (32) when $e_x(U^0)$ takes up the particular values

$$e_{xij}(U^0) = 1 \text{ when } i = \alpha \text{ and } j = \beta; \quad e_{xij}(U^0) = 0 \text{ otherwise}$$

The usual compatibility conditions then lead to the set of macroscopic equations

$$\mathrm{div}_x\langle\sigma^0\rangle = 0; \quad \langle\sigma^0\rangle = C_{ref}^* : e_x(U^0) \tag{35}$$

where $\langle . \rangle = \frac{1}{|\Omega|}\int_\Omega (.) d\Omega$ is the spatial averaging operator, and C_{ref}^* is a fourth-order tensor comprised of the equivalent macroscopic moduli, which accounted for the material properties of elastic and viscoelastic phases, and their respective topologies. Its components are given by

$$\begin{aligned}
C_{ref}^{*ijkl} = (1-n)a^{ijkl} + \frac{(1-n)a^{ijmn}}{|\Omega_s|}\int_{\Omega_s} e_{ymn}(\chi_{ref}^{kl}) d\Omega + 2nM_{ref}^*\delta_{ik}\delta_{jl} \\
+ \frac{n}{|\Omega_f|}\left[2M_{ref}^*\int_{\Omega_f} e_{yij}(\chi_{ref}^{kl}) d\Omega + \delta_{ij}\int_{\Omega_f} \tau_{ref}^{kl} d\Omega\right]
\end{aligned} \tag{36}$$

The above relation also defines the macroscopic moduli C^{*ijkl} at any other temperature θ, upon replacement of M_{ref}^* by $M^*(\omega,\theta)$.

4.3. Mechanical dissipation in terms of macroscopic variables

Since $d(\dot{U}) = e(i\omega U)$, the instantaneous mechanical power (in part reversible, in part dissipative) is locally given by $S = Re[\sigma] : Re[e(i\omega U)]$ in both solid and fluid phases. Integrating over Ω_s and Ω_f, taking into account the respective forms of σ at zero order, we obtain the following space average of the total mechanical power Π, entirely in terms of macroscopic variables

$$\langle\Pi\rangle = Re[C_{ref}^* e_x(U^0)] : Re[e_x(i\omega U^0)] \tag{37}$$

depending exclusively on the macroscopic quantities C^*_{ref} and U^0. Noting $U^0(x,t) = u^0(x,t)e^{i(\phi+\omega t)}$ (u^0 real), and splitting C^*_{ref} into its real and imaginary parts, C^r_{ref} and C^i_{ref}, we arrive at the following form of $\langle \Pi \rangle$ after a little simplification

$$\langle \Pi \rangle = \omega e(u^0) : \left\{ C^i_{ref} \sin^2(\phi + \omega t) - C^r_{ref} \frac{\sin(2(\phi + \omega t))}{2} \right\} : e(u^0) \tag{38}$$

The second term fluctuates around a zero average value and corresponds actually to the reversible elastic work. Hence the mechanical dissipative power in terms of macroscopic variables is

$$\langle S \rangle = \omega \sin^2(\phi + \omega t) e(u^0) : C^i_{ref} : e(u^0) \tag{39}$$

This expression is consistent with (24), the factor $2M_i$ at the microscopic level being replaced by C^i_{ref} at the macroscopic level. Note that heat generated by $\langle S \rangle$ should in principle modify the macroscopic moduli C^* through the temperature-dependent modulus $M^*(\omega, \theta)$ of the viscoelastic phase, while the isothermal description (35) and (36) does not take this effect into account.

4.4. Limits of validity of the isothermal description

The description given above has been validated experimentally by Boutin et al. (1995). However, on account of the thermal sensitivity of the material ($|\delta C^*/C^*| \sim 5$ %/°C in the case of bituminous concrete), and the heat energy accumulated at the end of a large number of cycles (typically over a million in a fatigue test of bituminous concrete), a temperature rise of a few degrees can be expected, and thermal-softening effects must be considered. Note that such effects were simulated by Piau (1989), and experimentally observed by Doubbaneh (1995).

To account for the thermal-softening effects on the mechanical behaviour, the thermal problem as defined in Section 3.2 has to be considered, taking notably into account heat generated by mechanical dissipation. In order to arrive at an entirely macroscopic description, the first step to be taken is to seek for a 'homogenised' version of the thermal problem, which allows definition of the equivalent specific heat and thermal conductivity, taking into account a macroscopic heat source similar to expression (39).

The thermal problem is to be solved simultaneously with the mechanical problem. At each stage, the temperature field θ so found is incorporated in the mechanical problem to update the values of the temperature-dependent mechanical parameters. Conversely, the latter information is used to update the heat source term.

In the forthcoming sections, we will begin with a detailed treatment of the thermal problem of a heterogeneous medium, distinguishing the different situations encountered, which will then be followed by an analysis of the coupled thermomechanical problem.

5. Space–time homogenisation of the thermal problem

5.1. The physics of thermal conduction in heterogeneous media

The physical process of thermal conduction in a heterogeneous medium is hereafter described. At small times, heat energy generated locally and non-uniformly in the viscoelastic phase creates a non-uniform temperature field of small amplitude, with spatial and temporal oscillations due to the harmonic *excitation* and the *microstructure*. Progressively, the local gradients flatten out by diffusion, while an average temperature rise becomes distinguishable.

At large times, the temperature field is macroscopically homogeneous across the local heterogeneities, local spatial fluctuations around the mean temperature profile being then negligible. Moreover, temporal oscillations are at this stage an order of magnitude lower than the current temperature, which evolves progressively.

Temperatures tend progressively towards steady-state conditions if the boundary conditions are not adiabatic everywhere and the source is quasi-constant and bounded.

5.2. Scale definition

For the problem we are interested in, the microscopic space-scale is naturally imposed by the size l of the heterogeneities of the material, while the time-scale is defined by the period t_e of the harmonic loading conditions ($t_e = 2(\pi/\omega)$.

On the other hand, one can always choose reference values of time $\tilde{t}$, length $\tilde{l}$, and temperature $\tilde{\theta}$ in such a way that, estimated with these characteristic values, the three terms in the heat equation, namely: the inertial, conductive and the source term, are all of the same order. In other words

$$O\left(\frac{\rho C\tilde{\theta}}{\tilde{t}}\right) = O\left(\frac{k\tilde{\theta}}{\tilde{l}^2}\right) = O(S) \tag{40}$$

In consequence, for the reference duration $\tilde{t}$, the reference length $\tilde{l}$ is identified with the heat front advance $\delta_{\tilde{t}} = (k\tilde{t})^{1/2}$ (with $k = \lambda/\rho C$) during $\tilde{t}$, and the reference temperature increase is given by $\tilde{\theta} = S\tilde{t}/(\rho C)$. The particular values $(\tilde{t}, \tilde{l}, \tilde{\theta})$ correspond to the natural choice of intrinsic reference values for the problem of heat transfer.

In other words, the inertial, conductive and the source terms are of the same order when pertinent space- and time-scales — corresponding to the characteristic time of evolution and the associated heat front avance — are adopted. In the following section, we will identify $\tilde{t}$ with the actual time, and $\tilde{l}$ with the current heat front advance $\delta_{\tilde{t}}$, and see how the relative magnitudes of the three terms may evolve in the course of loading, and the possible situations that may arise.

5.3. Different possible situations

On account of the above discussion, the analysis proceeds in the following manner: A) at the current time $\tilde{t}$, compare $\delta_{\tilde{t}}$ with l to see if a macroscopic spatial description is available; B) compare $\tilde{t}$ with t_e to see if a macrochronological temporal description is available.

Now rewrite the heat equation in local coordinates t and y, as defined in Section 3.3

$$\rho C\partial_t\theta - \mathrm{div}_y[\lambda\nabla_y(\theta)] = S \tag{41}$$

The relative order of magnitude of the three terms, expressed in local coordinates, is then

$$\frac{S}{\rho C\partial_t\theta} = O\left(\frac{S}{\rho C\theta/t_e}\right) = O\left(\frac{t_e}{\tilde{t}}\right) \tag{42}$$

$$\frac{S}{\mathrm{div}_y[\lambda\nabla_y(\theta)]} = O\left(\frac{S}{\lambda\theta/l^2}\right) = O\left[\left(\frac{l}{\delta_{\tilde{t}}}\right)^2\right] \tag{43}$$

on account of (16) and (17). Since physically, the temperature oscillations at any point cannot be 'faster' than the periodic fluctuation of the source itself, an observation time much shorter than t_e is inadequate for our problem. Hence, only two cases need to be distinguished

$$\tilde{t} = O(t_e) \quad \text{or} \quad \tilde{t} \gg t_e$$

For each, we have to compare $\delta_{\tilde{t}}$ with l for the existence of a macroscopic space description. There are thus four different cases to be considered, depending on the size of the heterogeneities, the thermal properties and the excitation frequency. We will briefly examine the qualitative results here below and leave the details of the analysis to Annexe A.

Case i: $\delta_{\tilde{t}}/l \leq O(1)$, $\tilde{t} = O(t_e)$

In this first case, the duration of observation is of the same order as the period of the source, hence only one time-scale is pertinent — the one defined by the period t_e of the mechanical load. Temperature rises take place with significant oscillations, and of a period comparable to the observation time, around the still weak current values (cf. *figure 2*). The fact that the heat front advance $\delta_{\tilde{t}}$ is still less than, or of the order of the size of heterogeneities l means that spatial temperature distribution is non-uniform, dominated by the source distribution. An adequate space–time description of this case can only be performed with local variables (y, t).

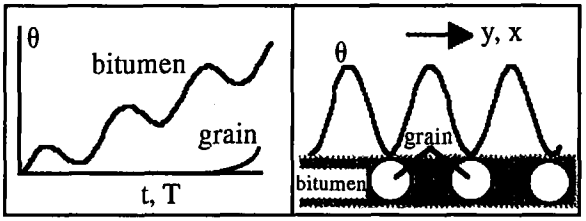

Figure 2. Space–time evolution of θ in Case i.

Case ii: $\delta_{\tilde{t}}/l \leq O(1)$, $\tilde{t} \gg t_e$

This second case corresponds to an observation time $\tilde{t}$ that is much longer than the period of excitation. A progressive temporal evolution profile can be distinguished, which can be described by the macro-chronological time-scale $\tilde{t}$. The fact that $\delta_{\tilde{t}}$ is less than or in the order of l means that the temperature field is spatially heterogeneous (cf. *figure 3*), and the local variable y must be retained for a pertinent spatial description (case of high frequency, low diffusivity, large-size heterogeneities).

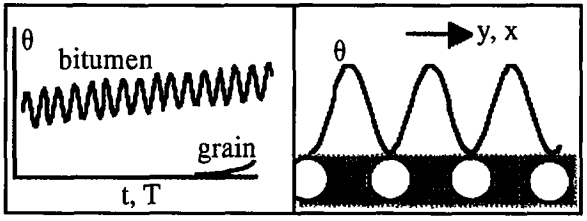

Figure 3. Space–time evolution of θ in Case ii.

We now consider cases $\delta_{\tilde{t}} \gg l$.

Case iii: $\delta_{\tilde{t}} \gg l$, $\tilde{t} = O(t_e)$

The advance of heat front $\delta_{\tilde{t}}$ is in this third case substantially larger than microstructural size l, even at small times (case of low-frequency excitation, high diffusivity, small heterogeneities or their combinations). In other words, temperatures tend to uniformise amongst local heterogeneities (cf. *figure 4*), and a pertinent macroscopic scale x exists, with a corresponding characteristic dimension $\delta_{\tilde{t}}$ suitably larger than l ($\delta_{\tilde{t}}/l \geq O(\varepsilon^{-1})$). On the other hand, temporal oscillations have only occurred for a few periods, and no pertinent macrochronological time description is yet available.

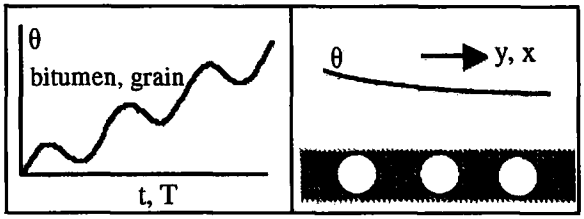

Figure 4. Space–time evolution of θ in Case iii.

Case iv: $\delta_{\tilde{t}} \gg l,\ \tilde{t} \gg t_e$

This is the most 'ideal' case, the irregularities in the temporal and spatial evolutions tend to be negligible. An average temperature profile can be distinguished, which increases progressively (cf. *figure 5*), and can be described entirely by macroscopic space–time variables.

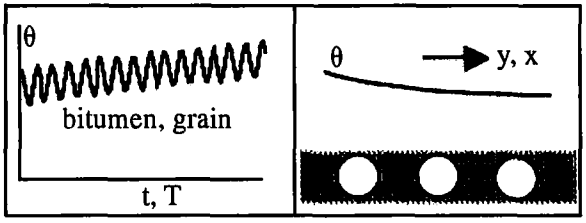

Figure 5. Space–time evolution of θ in Case iv.

The following table summarises the types of space–time description according to the scale factors.

Table I. Types of space–time description according to the scale factors.

		$\varepsilon_t = \dfrac{t_e}{\tilde{t}}$	
		$\varepsilon_t = O(1)$	$\varepsilon_t \ll 1$
$\varepsilon_1 = l/\delta_{\tilde{t}}$	$\varepsilon_1 = O(1)$	*Case i* (y,t) $\mathrm{div}_y[\lambda(\nabla\theta(y,t))] = \rho C\partial_t\theta(y,t) - S(y,t)$	*Case ii* (y,T) $\mathrm{div}_y[\lambda(\nabla_y\theta(y,T))] = \rho C\partial_T\theta(y,T) - \{S\}(y,T)$
	$\varepsilon_1 \ll 1$	*Case iii* (x,t) $\mathrm{div}_x[\lambda_M\nabla_x\theta(x,t)] = \langle\rho C\rangle\partial_t\theta(x,t) - \langle S\rangle(x,t)$	*Case iv* (x,T) $\mathrm{div}_x[\lambda_M\nabla_x\theta(x,T)] = \langle\rho C\rangle\partial_T\theta(x,T) - \langle\{S\}\rangle(x,T)$

Note: λ_M = macroscopic thermal conductivity, given by Eq. (A10), $\{S\}$ = time-average of S over a period $(t, t+t_e)$.

The above descriptions have been obtained under the most general assumptions. In particular situations, some of the terms may degenerate according to the specific loading conditions and the boundary conditions, leading to further simplifications. For example, a stationary state is reached at large time if the source is independent of the macrochronological time-scale and the boundary conditions are non-adiabatical (at least over part of the boundary) and time-independent.

5.4. Relation between the space-scale and time-scale factors

In order to treat all possible cases, it was assumed in the above analysis that the time-scale factor $\varepsilon_t = t_e/\tilde{t}$ and the space-scale factor $\varepsilon_1 = l/\delta_{\tilde{t}}$ were independent. However, for a given material and a fixed value of excitation frequency, these two scale factors are clearly not independent, on account of the equality $\delta_{\tilde{t}} = (k_M \tilde{t})^{1/2}$, hence

$$\frac{\varepsilon_t}{\varepsilon_1^2} = \frac{t_e}{\tilde{t}} \frac{k_M \tilde{t}}{l^2} = \frac{k_M t_e}{l^2} = \left(\frac{\text{heat front advance within one period } t_e}{\text{characteristic grain size}} \right)^2 \tag{44}$$

For the particular example of bituminous concrete ($l \approx 1\,\text{mm}$, $k_M = \lambda_M/\langle \rho C \rangle \approx 1\,\text{mm}^2/\text{s}$) subject to cyclic load tests at frequencies of $1 - 10$ Hz (hence $t_e = 0.1 - 1$ s), we have $k_M t_e/l^2 = O(1)$. Thus

$$\varepsilon_t \approx \varepsilon_1^2 \tag{45}$$

Physically, this means that when the temporal evolution reaches a state such that an average temperature rise can be distinguished (ie. a macrochronological time description is possible), the spatial distribution of the temperature field is still irregular, and no meaningful spatial average temperature profile can yet be distinguished. Only at still larger times, when $l/\delta_{\tilde{t}} = O(\varepsilon)$ and $t_e/\tilde{t} = O(\varepsilon^2)$, will a macroscopic space description be possible. In other words, as far as fatigue tests of bituminous concrete are concerned, we would normally encounter the following situations in the respective order

$$\text{Case i} \rightarrow \text{Case ii} \rightarrow \text{Case iv-b}$$

Other scenarios could effectively be encountered under different situations, for example a different material with different microstructural sizes, different thermomechanical properties and a different excitation frequency, where ε_1 and ε_t would be related by a different relationship.

6. Space–time homogenisation of the coupled thermomechanical problem

Having obtained a macroscopic description of the mechanical problem and that of the thermal problem separately, we are now in a position to treat the 'complete' problem, taking into account the coupling effects due to thermosensitivity, namely

$$\frac{\partial ||M^*||}{\partial \theta} < 0 \tag{46}$$

in our analysis. We will first review the space homogenisation taking into account (46), and then proceed onwards to obtain an entirely macroscopic description after another homogenisation with respect to time.

6.1. Space homogenisation

The previous description given in Section 4 has now to be revised, taking into account the temperature dependency of the complex modulus. Other assumptions adopted for the description of isothermal behaviour still hold. As before, we assume, to start with, that macroscopic space–time-scales exist. The necessary conditions will be reviewed after the solution process.

Denote by $\delta\theta = \theta^0 + \varepsilon\theta^1 + \varepsilon^2\theta^2 \ldots$ the temperature deviation from its initial reference value θ_{ref}. For 'small' temperature variations, the temperature-dependent complex modulus of the viscoelastic phase can be approximated by the first term in the Taylor series expansion

$$M^*(\omega, \theta) \sim M^*(\omega, \theta_{ref}) + A^*(\omega, \theta_{ref})(\theta^0 + \varepsilon\theta^1 + \ldots) \tag{47}$$

where $A^*(\omega,\theta_{ref}) = \partial_\theta M^*(\omega,\theta_{ref})$ expresses the thermal sensitivity of the material. To simplify, we will simply write A^*. The intensity of spatial fluctuations of M^* at zero order depends therefore on that of θ^0. Due to fluctuations of M^* the set of isothermal equations (31) have to be revised to

$$\begin{aligned}
&\mathrm{div}_y[a.e_y(U_s^0)] = 0 && \text{in } \Omega_s \\
&\mathrm{div}_y[(M_{ref}^* + A^*\theta^0)e_y(U_f^0)] = 0 && \text{in } \Omega_f \\
&a.e_y(U_s^0) = 2(M_{ref}^* + A^*\theta^0)e_y(U_f^0) && \text{on } \Gamma \\
&U_s^0 = U_f^0 && \text{on } \Gamma \\
&\mathrm{div}_y(U_f^0) = 0 && \text{in } \Omega_f
\end{aligned} \tag{48}$$

which is formally the same system as in (31), with M_{ref}^* replaced by $M_{ref}^* + A^*\theta^0$ – with the important difference that spatial and temporal fluctuations of θ (Ω and t_e periodic) pass on to the modulus $M^*(x,y,T,t) = M_{ref}^* + A^*\theta^0$ in the present case. Notwithstanding, we still arrive at the same conclusion that $U_s^0 = U_f^0 = U^0(x,T,t)$ is independent of y, despite the space fluctuations of θ^0.

The same modification affects the system of an order higher

$$\begin{aligned}
&\mathrm{div}_y[a : (e_x(U^0) + e_y(U_s^1))] = 0 && \text{in } \Omega_s \\
&-\nabla_y P^0 + 2\mathrm{div}_y[(M_{ref}^* + A^*\theta^0)(e_x(U^0) + e_y(U_f^1))] = 0 && \text{in } \Omega_f\,. \\
&a : [e_x(U^0) + e_y(U_s^1)] \cdot N = (-P^0 1 + 2(M_{ref}^* + A^*\theta^0)[e_x(U^0) + e_y(U_f^1)]) \cdot N && \text{on } \Gamma \\
&U_s^1 = U_f^1 && \text{on } \Gamma \\
&\mathrm{div}_x(U^0) + \mathrm{div}_y(U_f^1) = 0 && \text{in } \Omega_f
\end{aligned} \tag{49}$$

which admits the same kind of solution as before, except that it now depends implicitly on the value of θ^0

$$U^1 = u^1(x,T,t) + \chi^{\alpha\beta}(y)e_{x\alpha\beta}(U^0) \tag{50}$$

$$P^0 = \tau_{\alpha\beta}(y)e_{x\alpha\beta}(U^0) \tag{51}$$

and the macroscopic description

$$\mathrm{div}_x\langle\sigma^0\rangle = 0; \quad \langle\sigma^0\rangle = C^* : e_x(U^0) \tag{52}$$

where similar to Section 4.2, $\chi^{\alpha\beta}$ and $\tau_{\alpha\beta}$ are the particular solutions of the system (49) when $e_{xij}(U^0) = 1$ for $i = \alpha$ and $j = \beta$ and $e_{xij}(U^0) = 0$ otherwise, and C^* is the tensor of the equivalent macroscopic moduli

$$\begin{aligned}
C^{*ijkl} = (1-n)a^{ijkl} + \frac{(1-n)a^{ijmn}}{|\Omega_s|}\int_{\Omega_s} e_{ymn}(\chi^{kl})d\Omega + 2n(M_{ref}^* + A^*\theta^0)\delta_{ik}\delta_{jl} \\
+\frac{n}{|\Omega_f|}\left[2(M_{ref}^* + A^*\theta^0)\int_{\Omega_f} e_{yij}(\chi^{kl})d\Omega + \delta_{ij}\int_{\Omega_f}\tau^{kl}d\Omega\right]
\end{aligned} \tag{53}$$

The thermomechanical coupling intervenes here by the explicit presence of the term $M_{ref}^* + A^*\theta^0$ and the implicit dependence of $\chi^{\alpha\beta}$ and $\tau_{\alpha\beta}$ on θ^0.

Here again, the instantaneous mechanical power is locally given by $\Pi = Re[\sigma] : Re[e(i\omega U^0)]$. The space average $\langle\Pi\rangle$ is formally similar to (38). Using the notation

$$U^0(x,T,t) = \mathcal{U}^0(x,T)e^{i\omega t} = u^0(x,T)e^{i\phi(x,T)}e^{i\omega t}; \quad C^* = C_r + iC_i \ (C_r \text{ and } C_i \text{ real}) \tag{54}$$

where $u^0 = ||U^0||$ is the 'real' displacement amplitude and ϕ the phase-lag, the instantaneous power $\langle \Pi \rangle$ can be written as

$$\langle \Pi \rangle = \omega e(u^0) : \left\{ C_i \sin^2(\phi + \omega t) - C_r \frac{\sin(2(\phi + \omega t))}{2} \right\} : e(u^0) \tag{55}$$

and the part dissipated

$$\langle S \rangle = \omega \sin^2(\phi + \omega t) e(u^0) : C_i : e(u^0) \tag{56}$$

Contrary to (38) and (39) however, C_r and C_i evolve with time due to thermosensitivity.

6.2. Time homogenisation

In the forthcoming sections, we will only retain the first-order terms θ^0 and U^0. To simplify notation, the exponent 'o' will be dropped. On a finite volume V, bounded by a closed surface ∂V (*figure* 1), the spatially homogenised mechanical boundary problem is defined by the following set of equations

$$\begin{aligned} &\operatorname{div}[C^* : e(U)] = 0 \quad \text{in } V \\ &\text{Case 1.} \quad U = U^d(x,T)e^{i\omega t} \quad \text{on } \partial V_U; \quad C^* : e(U) \cdot N = 0 \quad \text{on } \partial V_\sigma \ \text{(displacement controlled)} \\ &\text{Case 2.} \quad C^* : e(U) \cdot N = \sigma^d(x,T)e^{i\omega t} \quad \text{on } \partial V_\sigma; \quad U = 0 \quad \text{on } \partial V_U \ \text{(stress controlled)} \end{aligned} \tag{57}$$

where for generality we have supposed that the imposed displacements and stresses $U^d e^{i\omega t}$ and $\sigma^d e^{i\omega t}$ vary on both time-scales. In practical cases, they usaually do not depend on T. To simplify the presentation, we will suppose either displacement-controlled (Case 1) or stress-controlled fatigue tests (Case 2). Generalisation to simultaneous existence of both types of boundary conditions can be achieved by superposition. Linearity of the equations clearly suggests a solution of the form $U = \mathcal{U}(x,T)e^{i\omega t} = ue^{i\phi}e^{i\omega t}$, u real and $\mathcal{U}(x,T) = ue^{i\phi}$ being the complex amplitude of the oscillation varying on the macro-chronological time-scale, solution of the following system obtained from (57)

$$\begin{aligned} &\operatorname{div}[C^* : e(\mathcal{U}(x,T))] = 0 && \text{in } V \\ &\text{Case 1.} \quad \mathcal{U}(x,T) = U^d(x,T) && \text{on } \partial V_U; \quad C^* : e(\mathcal{U}) \cdot N = 0 \quad \text{on } \partial V_\sigma \\ &\text{Case 2.} \quad C^* : e(\mathcal{U}(x,T)) = \sigma^d(x,T) && \text{on } \partial V_\sigma; \quad \mathcal{U} = 0 \quad \text{on } \partial V_U \end{aligned} \tag{58}$$

Time does not intervene explicitly in (58), but we need the temperature field at each instant in order to calculate C^*. Denoting by $\{\}$ the temporal averaging operator, defined by

$$\{ . \} = \frac{1}{t_e} \int_\tau^{\tau + t_e} (.) d\tau$$

and on account of the relation $t_e = 2\pi/\omega$, the macroscopic source $\langle \{S\} \rangle$ can be simplified to

$$\langle \{S\} \rangle = \frac{\omega}{2} e(u) : C_i : e(u) \tag{59}$$

which is a quadratic function of $e(u)$, depending only on the macroscopic coordinates x and T.

The homogenised thermal problem is thus defined by

$$\begin{aligned} &\operatorname{div}[\lambda_M \nabla\theta] = \rho C \partial_T \theta - \langle \{S\} \rangle \quad \text{in } V \\ &\theta = \theta^d(x) \quad \text{on } \partial V_\theta \quad \text{(imposed temperature)} \\ &-\lambda \nabla\theta \cdot N = q^d(x) \quad \text{on } \partial V_q \quad \text{(imposed heat flux)} \end{aligned} \tag{60}$$

The last equations (58)–(60) define a completely macroscopic description of the coupled boundary problem through a set of nonlinear partial differential equations involving only macroscopic coordinates x and T. Its solution gives directly the long-term 'drifts' of temperature and displacement amplitudes.

7. Domain of validity

The remarkably simple form of the final system of Eqs (58)–(60) deserves a few comments. Notably, the validity of the macroscopic description derived is subject to specific conditions.

Recalling the approximative equality $||\Delta M^*/M^*_{ref}|| = ||A^*\Delta\theta/M^*_{ref}||$, we deduce that $||\Delta M^*/M^*_{ref}|| < \varepsilon$ whenever the temperature increase is less than a critical value defined by $\theta_{crit} = \varepsilon||M^*_{ref}/A^*||$. In other words, thermal effects on mechanical properties are negligible as long as $\theta < \theta_{crit}$. On account of the thermal power S and the volumetric heat capacity ρC, this leads to the definition of a critical time defined by $t_{crit} \doteq \rho C\theta_{crit}/S$, such that $t < t_{crit}$ implies $\theta < \theta_{crit}$. With reference to the definition of t_{crit} and θ_{crit}, the following situations can be distinguished.

i) $t_{crit} \gg t_e$:

for $t \ll t_{crit}$, we have necessarily $\theta \ll \theta_{crit}$, and the isothermal description applies whatever the distribution may be of θ within the RVE. Whereas for $t \geq t_{crit}$, we have necessarily $\theta > \theta_{crit}$; the inequality $t_{crit} \gg t_e$ implies that θ already varies on a macrochronological time-scale when t sweeps across t_{crit} (i.e. when θ bypasses θ_{crit}, and the macroscopic description [Eqs (43)–(45)] applies. Hence we have a smooth transition from a macroscopic isothermal behaviour at small times (described by a constant complex modulus M^*_{ref}), to a coupled behaviour (M^* varies with θ, therefore with time) when t goes beyond t_{crit}.

ii) $t_{crit} \leq t_e$ or $t_{crit} \approx t_e$:

in this case, the duration during which thermal effects are negligible ($t < t_{crit}$) is smaller or of the same order as a loading cycle. We are then in a very particular situation: the mechanical properties evolves significantly even within a single loading cycle. In such a case, the concept of a complex modulus — which supposes a purely isothermal harmonic excitation at the stationary regime — can no longer be applied [hypothesis behind a harmonic solution (3) breaks down], and the overall behaviour is highly non-linear. Note however that for materials commonly encountered in civil engineering and for ordinary loading conditions (frequency, strain amplitude and temperature), this last case is never met in practice.

In order to illustrate the above discussion, let us consider the case of an isotropic bituminous concrete sample subjected to a fatigue test at a frequency of 10 Hz, with a strain amplitude of 10^{-4}. At this frequency, δ_{te} is around 0.2 mm. Moreover, at ambient temperature with typical thermophysical properties, the amplitude and the dissipative part of the macroscopic complex shear modulus are respectively in the order of 3000 and 1000 MPa, and the thermosensitivity $||A^*||$ is around 150 MPa/°C. The value of θ_{crit} is given by $||A^*\theta_{crit}/M^*_{ref}|| = 10^{-3}$ (if we choose a precision of $\varepsilon = 10^{-3}$) so that $\theta_{crit} \approx (10^{-3}\ 3000/150) = 0.02$°C. On acount of the strain amplitude, the thermal power dissipated leads to a temperature increase per cycle of around 1.5×10^{-5}°C. With this in mind, the evolution of a typical fatigue test can be described approximately as below

End of first cycle (0.1 s): $= 1.5 \times 10^{-5}$, and $||\Delta M^*/M^*_{ref}|| = 7.5 \times 10^{-7} \ll 10^{-3}$, therefore the isothermal description is valid.

After 100 cycles (10 s): $\theta = 1.5 \times 10^{-3}$°C, hence $||\Delta M^*/M^*_{ref}|| = 7.5 \times 10^{-5} \ll 10^{-3}$. While at this time, the temperature begins to unformise, since $\delta_{100te} = 2$ mm $\approx l$ (typical grain size of a few mm), there is still no incidence on the mechanical behaviour as the magnitude of θ is small ($\theta \ll \theta_{crit}$).

After 1000 cycles (100 s): $\theta = 0.015$°C, and $||\Delta M^*/M^*_{ref}|| = 7.5 \times 10^{-4}$. Thermal effects start to approach the critical threshold.

After 10^4 cycles (1000 s): $\theta = 0.15°C$, and $||\Delta M^*/M^*_{ref}|| = 7.5 \times 10^{-3} > 10^{-3}$. Mechanical softening due to internal heating becomes significant. Notice that we now have $\delta_{10^4 te} = 2$ cm $> l$, so that the temperature is practically constant in the unit cell.

These simple estimations will be completed by a 1-D example in the next section.

8. Multi-layered media: a 1-D example

In this section, the previous results are applied to a simple 1-D structure. Although the existence of such idealised media is hypothetical, this model does display efficiently the essential features of the above development. The original treatment was given by Boutin and Auriault (1990) assuming isothermal conditions, in which interested readers can find greater details.

8.1. Analytical formulation

Consider a stratified periodic medium consisting of alternating elastic (Ω_s) and viscoelastic (Ω_f) layers (*figure 6*). Both phases are homogeneous and isotropic, with thicknesses of $(1-n)h$ and nh respectively.

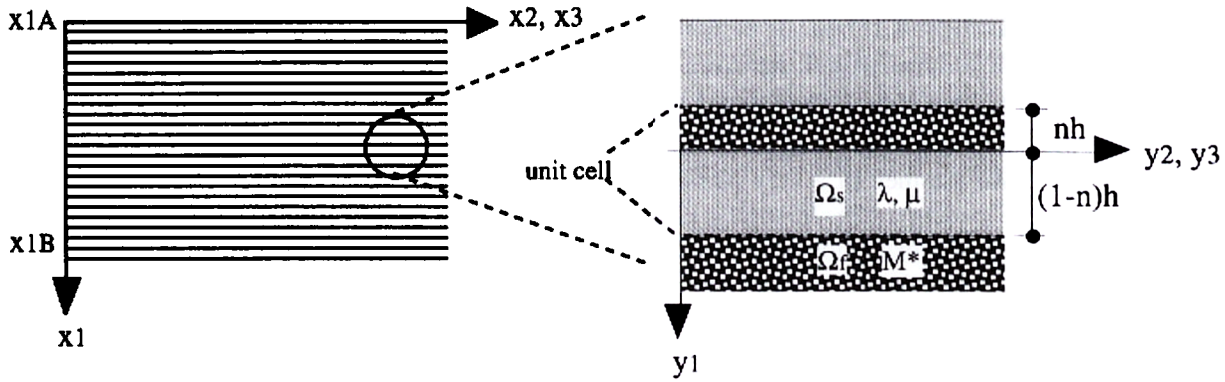

Figure 6. Geometry of the multi-layered medium.

The problem is to find the particular solutions χ^{jk} which give in turn the first-order displacement U^1. On account of the symmetry, the periodicity and the static equilibrium requirements, U^1 is of the form

$$U^1_{si} = a_i y_1 + b_i; \quad U^1_{fi} = a'_i y_1 + b'_i$$

Only the coefficients a_i and a'_i are of interest, since b_i and b'_i give no contribution to the strains. According to Boutin and Auriault (1990)

$$a_1 = \frac{n}{1-n}(e_{11} + e_{22} + e_{33}); \quad a_2 = -2e_{12}nK^*; \quad a_3 = -2e_{13}nK^*$$
$$a'_1 = -(e_{11} + e_{22} + e_{33}); \quad a'_2 = 2e_{12}(1-n)K^*; \quad a'_3 = 2e_{13}(1-n)K^*$$
$$K^* = \frac{\mu - M^*}{n\mu + (1-n)M^*}$$

where $e_{ij} = e_{xij}(U^0)$ is the macroscopic strain tensor of the zero-order displacement, while the fluid pressure at zero order is given by

$$P^0 = 2(\mu - M^*)e_{11} + \frac{\lambda + 2(n\mu + (1-n)M^*)}{1-n}(e_{11} + e_{22} + e_{33}) \quad .$$

Identification term by term allows the determination of the particular solutions χ^{jk}, and finally the complex tensor C^* relating the macroscopic strain to the macroscopic stress. Putting the stress and strain tensors in vectorial form, respectively $\sigma = \{\sigma_{11}, \sigma_{22}, \sigma_{33}, \sigma_{23}, \sigma_{31}, \sigma_{12}\}$ and $\varepsilon = \{\varepsilon_{11}, \varepsilon_{22}, \varepsilon_{33}, 2\varepsilon_{23}, 2\varepsilon_{31}, 2\varepsilon_{12}\}$, C^* can be expressed in matrix form as follows

$$C^* = \begin{bmatrix} \frac{\lambda+2\mu}{1-n} & \frac{\lambda+2n\mu}{1-n} & \frac{\lambda+2n\mu}{1-n} & 0 & 0 & 0 \\ & \frac{\lambda+2\mu}{1-n} + 4n(M^*-\mu) & \frac{\lambda+2n^2\mu}{1-n} + 2nM^* & 0 & 0 & 0 \\ & & \frac{\lambda+2\mu}{1-n} + 4n(M^*-\mu) & 0 & 0 & 0 \\ & & & (1-n)\mu + nM^* & 0 & 0 \\ & \text{SYM} & & & \frac{\mu M^*}{n\mu + (1-n)M^*} & 0 \\ & & & & & \frac{\mu M^*}{n\mu + (1-n)M^*} \end{bmatrix}$$

In particular, the complex shear modulus $(1-n)\mu + nM^*$ corresponds to the sum of the stiffnesses, taking into account the respective volume fractions, when shearing occurs in the plane perpendicular to the stratification (i.e. σ_{23}), while $\mu M^*/[n\mu + (1-n)M^*)]$, the inverse of $n/M^* + (1-n)/\mu$, represents an addition of flexibilities when shearing occurs in a plane parallel to the stratification (ie. σ_{12} or σ_{13}). These correspond to classic parallel and series structural mechanisms.

8.2. Particular case of pure shear and undeformable solid phase

For illustrative purposes, consider a state of pure shear in which only σ_{12} and e_{12} are non-zero. Thus, the only non-zero displacement component is in the y_2 direction, namely: $U^1_{s2} = -2nK^* e_{12} y_1$ and $U^1_{f2} = 2(1-n)K^* e_{12} y_1$, leading to the following forms of the strain tensor components

$$e_x(U^0) = \begin{bmatrix} 0 & e_{12} & 0 \\ e_{12} & 0 & 0 \\ 0 & 0 & 0 \end{bmatrix};$$

$$e_y(U^1_s) = \begin{bmatrix} 0 & -nKe_{12} & 0 \\ -nKe_{12} & 0 & 0 \\ 0 & 0 & 0 \end{bmatrix}; \quad e_y(U^1_f) = \begin{bmatrix} 0 & (1-n)Ke_{12} & 0 \\ (1-n)e_{12} & 0 & 0 \\ 0 & 0 & 0 \end{bmatrix}$$

which give, upon superposition, the zero-order strains within the elastic ($e^0_s = e_x(U^0) + e_y(U^1_s)$) and viscoelastic ($e^0_f = e_x(U^0) + e_y(U^1_f)$) phases, as illustrated in *figure 7*. In other words, while the macroscopic displacement is correctly described by the zero-order term U^0 alone, local fluctuations being of the order $O(\varepsilon)$, its macroscopic derivative $e_x(U^0)$ only indicates the average strains. A correct description of the stresses, which depends on the 'true strains', must take into account the first-order displacements independently of the scale factor.

In this form the problem is still complicated since the dependence of M^* on θ is itself complex. A particularly interesting limiting case presents when the stiffness of the solid phase tends towards infinity (undeformable). This case is a fairly good approximation for bituminous concrete for which the order of $||\mu/M^*||$ is around 100.

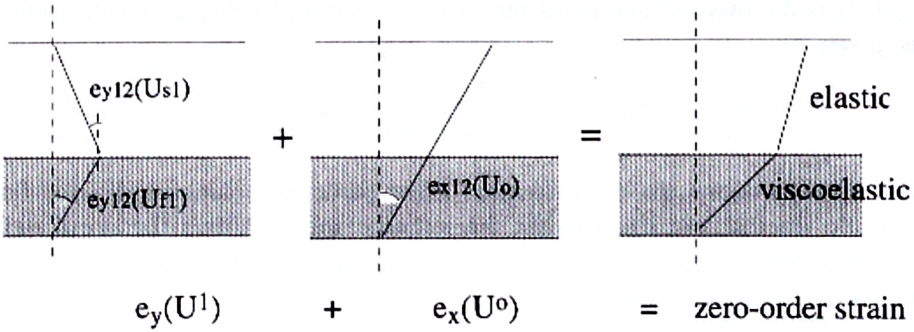

Figure 7. Decomposition of zero-order strain into a macroscopic and a localised component.

When $\mu \to \infty$, we have

$$K^* \to \frac{1}{n}, \text{ thus } e_{y12}(U_s^1) \to -e_{12}, \text{ and } e_{y12}(U_f^1) \to \frac{1-n}{n} e_{12}$$

The local ('true') strain $e_x(U^0) + e_y(U^1)$, associated with a macroscopic average strain profile e_{12} is therefore given by

$$e_{s12} = 0 \text{ in the elastic phase}$$
$$e_{f12} = \frac{e_{12}}{n} \text{ in the viscoelastic phase}$$

On the other hand, the macroscopic harmonic shear flexibilities (coefficients $1/C_{55}^*$ and $1/C_{66}^*$) tend to their limiting value n/M^* as $\mu \to \infty$. This is illustrated in *figure 8*.

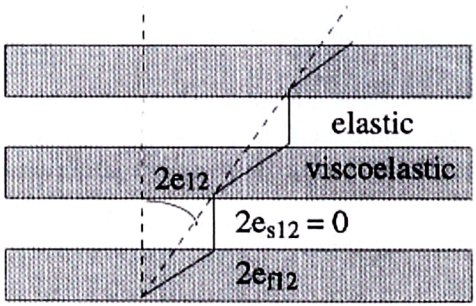

Figure 8. Shear strain in the elastic and viscoelastic layers, and the macroscopic average strain profile.

Thus, a macroscopic shear stress of σ_{12} induces a shear strain of $e_{f12} = \frac{1}{2M^*}\sigma_{12}$ in the fluid and zero shear strain in the solid, leading to a macroscopic shear strain of $e_{12} = \frac{n}{2M^*}\sigma_{12}$, on account of their relative thicknesses. Another important consequence is that the global response e_{12} is 'in phase' with the local response e_{f12}.

8.3. Mechanical dissipation (the heat source)

Consider a pure sinusoidal excitation, with $\sigma_{12} = \Sigma e^{i\omega t}$, which induces a sinusoidal response $e_{12} = (\gamma/2)e^{i(\omega t - \phi)}$ (Σ and γ both real), given by the equation $\sigma_{12} = 2C_{66}^* e_{12}$. Putting $M^* = ||M||e^{i\phi}$, we have

$$\Sigma = \frac{||M^*||}{n}\gamma$$

The macroscopic mechanical power is thus given by

$$\langle \Pi \rangle = Re[\sigma_{ij}]Re[i\omega e_{ij}] = Re\left[2\frac{M^*}{n}e_{12}\right]Re[i\omega e_{12}]$$

Using expressions involving Σ and γ, this can be simplified to

$$\langle \Pi \rangle = \omega\Sigma\gamma Re[e^{i\omega t}]Re[ie^{i(\omega t-\phi)}]$$

Taking the average over a period from t to $t + 2\pi/\omega$, and eliminating the reversible work gives the doubly-homogenised macrosocopic dissipation

$$\{\langle S \rangle\} = \frac{1}{2}\omega\Sigma\gamma\sin\phi$$

At a particular point in the medium, the relation $\Sigma = ||M^*||\gamma/n$ allows expression of $\{\langle S \rangle\}$ either in terms of the stress amplitude Σ or of the strain amplitude γ

$$\{\langle S \rangle\} = \frac{\omega\Sigma^2\sin\phi}{2||M^*||/n} = \frac{1}{2}\omega\frac{||M^*||}{n}\gamma^2\sin\phi = \frac{1}{2}\omega\frac{M_i}{n}\gamma^2$$

8.4. Boundary value problem with imposed stress

When a sinusoidal shear stress $\sigma_{12} = \Sigma e^{i\omega t}$ is applied on the upper free surface x_{1A} (*figure 6*), the equilibrium condition and the negligence of inertial effects impose a homogeneous stress field, which follows instantaneously the boundary traction without phase-lag. Taking into account the first form of $\{\langle S \rangle\}$, the uncoupled problem of thermal conduction to be solved is

$$\langle \rho C \rangle \partial_T\theta - \lambda_M\frac{\partial^2\theta}{\partial x^2} = \frac{n\omega\Sigma^2}{2}\frac{\sin[\phi(\theta)]}{||M^*(\theta)||} \quad \text{in } V$$

$$\text{(BC1)} \quad \theta = \theta^d(x) \quad \text{on } \partial V_\theta$$

$$\text{(BC2)} \quad -\lambda_M\frac{\partial\theta}{\partial x} = q^d(x) \quad \text{on } \partial V_q$$

Either (BC1) or (BC2) or mixed boundary conditions are admissible on $x = x_{1A}$, similarly for x_{1B}.

This is a well-defined, non-linear thermal conduction problem with the source term depending on the current temperature; it can be solved numerically by standard packages (using the Euler implicit scheme for example).

8.5. Numerical example

8.5.1. Material properties and loading

Consider a multi-layer medium of viscoelastic bitumen and undeformable solid, as shown in *figure 6*, with a total thickness of 10 cm ($x_{1A} = 0$, $x_{1B} = 10$ cm), consisting of alternating layers of bitumen of 1 mm and solid of 9 mm (i.e. $h = 1$ cm, $n = 0.1$), with the following properties.

Bitumen: see for example Huet (1963) for the time-frequency dependence of the bitumen modulus

$\lambda_f = 0.2$ W/m/°C; $(\rho C)_f = 2 \times 10^6$ J/m^3/°C

$M^*(\omega,\theta) = M^*[\omega\tau(\theta)] = \frac{M_\infty}{1+\delta(i\omega\tau(\theta))^{-h}+(i\omega\tau(\theta))^{-k}}$

$M_\infty = 2000$ MPa; $\delta = 4.3$; $h = 7.4$; $k = 0.27$; $f = 10$ Hz

$\tau(\theta) = \tau_{10}\ \text{Exp}[-\frac{C_1(\theta-10)}{C_2+\theta-10}]$; $\tau_{10} = 0.0021$ s; $C_1 = 20$; $C_2 = 150$°C

Grains: $\lambda_s = 1.4$ W/m/°C; $(\rho C)_s = 2 \times 10^6$ J/m^3/°C
subject to the following boundary and initial conditions

$$\theta(x_{1A}) = \theta(x_{1B}) = \theta_{ref} = 10°\text{C}$$
$$\theta(t = 0) = \theta_{ref} = 10°\text{C}$$

Equivalent homogeneous material properties:

$$\lambda_M = 0.875\ \text{W/m/°C}$$
$$\langle \rho C \rangle = 2 \times 10^6\ \text{J/m}^3\text{/°C}$$

where $1/\lambda_M = (1-n)/\lambda_s + n/\lambda_f$, λ_M being the conductivity perpendicular to the multilayers.

The classic representation of the complex modulus of bitumen M^* on the Cole–Cole plane is shown in *figure 9*, together with the locations of four particular values of M^* at respectively 10, 20, 35 and 60°C at 10 Hz. *Figure 10* shows the reduction of M_r, M_i (the real and imaginary parts of M^*) and $||M^*||$ with temperature, in the range of 10–70°C.

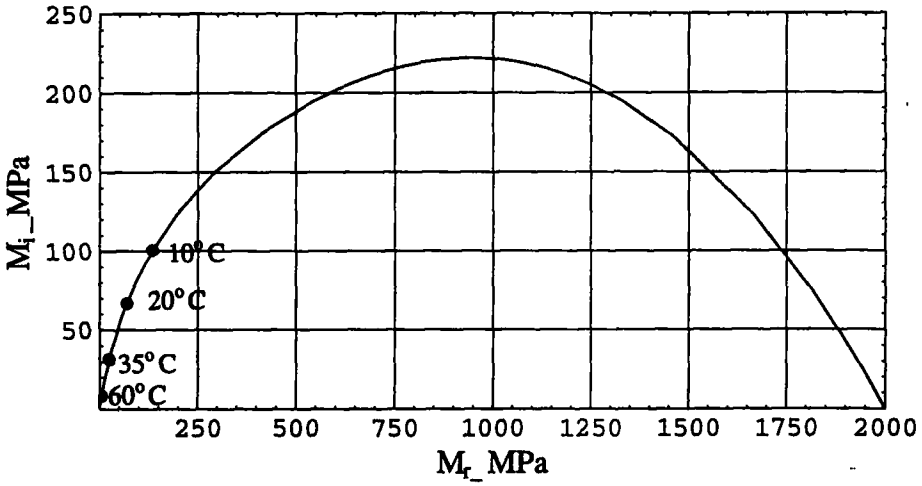

Figure 9. M_i versus M_r of the bitumen considered (Cole–Cole representation, complete spectrum and the portion for temperatures between 10–70°C)

Loading: a cyclic shear stress is applied to the surface at $x_1 = x_{1A}$. Quasi-static equilibrium implies that at all times, this boundary stress is followed by the shear stress at every point of the medium without delay. The amplitude and frequency of the applied shear stress are

$$\Sigma = 0.5\ \text{MPa}; \quad f = 10\ \text{Hz}$$

8.5.2. Numerical results and comments

A) Small time evolution, constant modulus: at small times, except at points close to the boundary, the boundary conditions are not felt (since the heat front advance δ_t is then of negligible magnitude: Case i). The periodical microstructure implies that the temperature field must be h-periodical, with maximum and mininum values occuring respectively in the middle of bitumen and solid layers, and zero heat flux at the same points. Analysis can therefore be restricted to a unit cell $-nh/2 < y_1 < (1-n)h/2$ (*figure 6*) with a volumetric power of $S_f = \omega\Sigma^2 \sin\phi/(2||M^*||)$ in the bitumen layer: $-nh/2 < y_1 < 0$. At small times, since the temperature

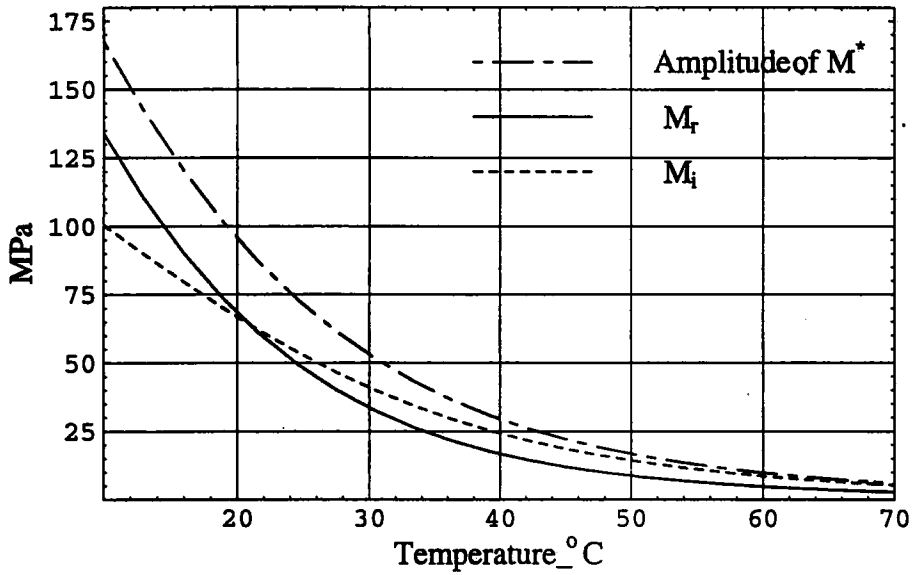

Figure 10. Reduction of $||M^*||$, $Re[M^*]$ and $Im[M^*]$ with temperature.

change is small, we can take, as a first approximation, $M^*(\theta) = M^*(\theta_{ref})$. At 10 °C, for the given properties of the bitumen, we have $||M^*|| = 168$ MPa, $M_r = 134$ MPa, and $M_i = 100$ MPa, leading to an initial thermal power of $S_f = 28138$ W/m^3 within the bitumen, the thermal power of the solid phase being taken to be zero.

Figure 11 plots the temperature evolution at the middle of solid (θ_s) and bitumen layers (θ_f). At very small times, when heat generated is still confined to the bitumen layer, (θ_f) rises very quickly according to $\theta_f = \theta_{ref} + tS_f/(\rho C)_f = 10 + 0.014t$, while (θ_s) remains at θ_{ref}. As a local temperature gradient appears,

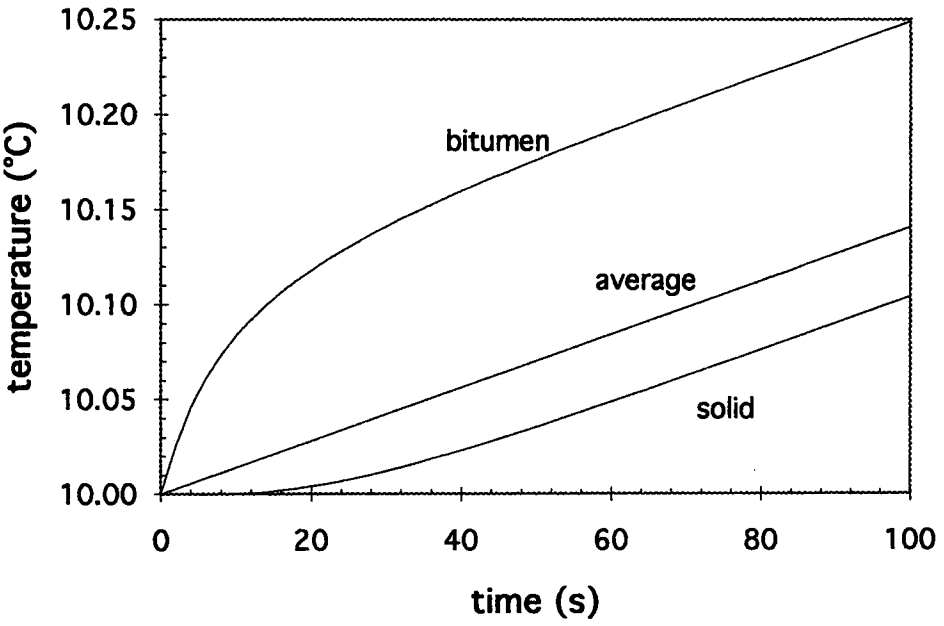

Figure 11. Small time temperature evolutions at middle layers of solid and fluid phases, compared to the global temperature rise due to a homogenised heat source.

heat is transferred to the adjacent solid layer in such a way that the curve (θ_f) flattens out, while (θ_s) begins to rise. After an initial duration of about 40 s (of which the characteristic diffusion time $\langle \rho C \rangle L^2/\lambda_s \approx 36$ s is a correct order of magnitude estimate), when heat generated is shared by both phases, both curves follow the same slope - that of the average temperature $\langle \theta \rangle = \langle \{S\} \rangle t/\langle \rho C \rangle + \theta_{ref}$. where $\langle \{S\} \rangle$ is the macroscopic volumetric thermal power given by $\langle \{S\} \rangle = n\{S_f\}$, taking into account the respective volume fractions.

B) Small time evolution, homogenised medium and source, changing modulus: if the reduction in stiffness due to a temperature rise is taken into account, a constant stress amplitude will lead to an increasing strain amplitude, thus the thermal power increases with time. The temperature increase will then be faster than in Case A above, as shown in *figure 12* below. The effect is largely non-linear, as the increased thermal power accelerates temperatures rises, which in turn enhances the stiffness loss. The negligence of boundary conditions, equivalent to an adiabatical condition here, will then lead to an artificial 'explosive' temperature rise.

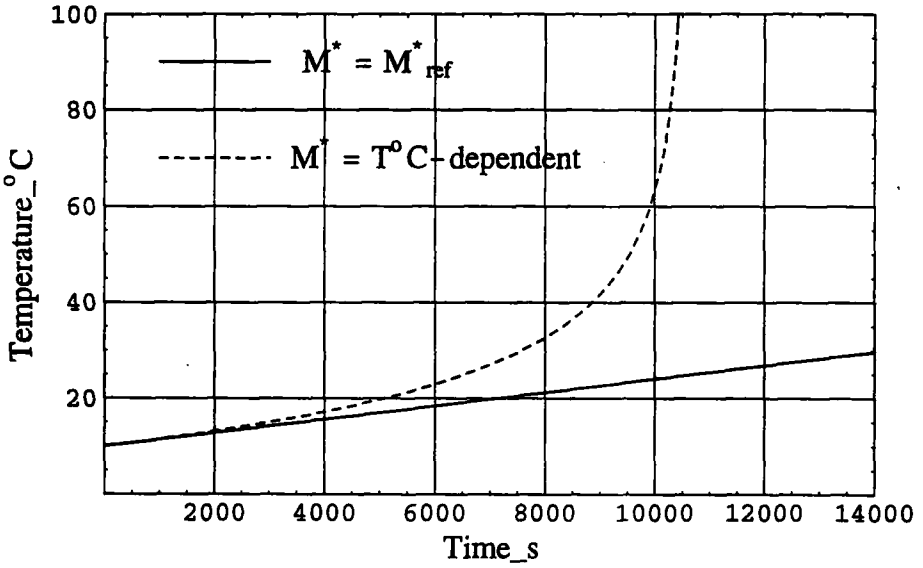

Figure 12. Homogenised temperature rises, with Case B: M^* temperature-dependent, compared to Case A: M^* temperature-independent.

C) Large time evolution, homogenised medium and source: at large times, the boundary conditions can no longer be neglected. For the particular case of fixed temperatures at x_{1A} and x_{1B}, the temperature field tends towards a stationary profile. This stationary profile is parabolic if the complex modulus remains at its initial value $M^*(\theta_{ref})$, leading thereby to a constant thermal power. The transient values now have to be found by solving the partial differential equations (Section 8.4), which is non-linear for the temperature-dependent modulus.

Evolutions in the temperature profile in both cases are plotted in *figure 13*. Close to each other at small times, when $M^*(\theta)$ is of little difference from its initial value $M^*(\theta_{ref})$, the two temperature fields tend to separate from each other at larger times, especially near the centre where larger temperature differences occur.

Figure 14 shows the profiles of M^* at different times, illustrating quantitatively the stiffness loss due to temperature. Again, the minimum of M^* occurs at the centre where θ is maximum, and converges to the ends where θ is fixed at θ_{ref}. Note that for a maximum temperature rise in the order of 4 °C in this example, and for a typical reduction of $||\Delta M^*/M^*|| = 7$ % per degree rise in temperature, this leads to a 28 % reduction in M^*. For constant applied stress, this stiffness loss leads to an increase in strains, as illustrated by *figure 15*. On account of $||C^*_{66}|| = ||M^*(10\ °C)||/n = 1680$ MPa, the initial strain amplitude is given by

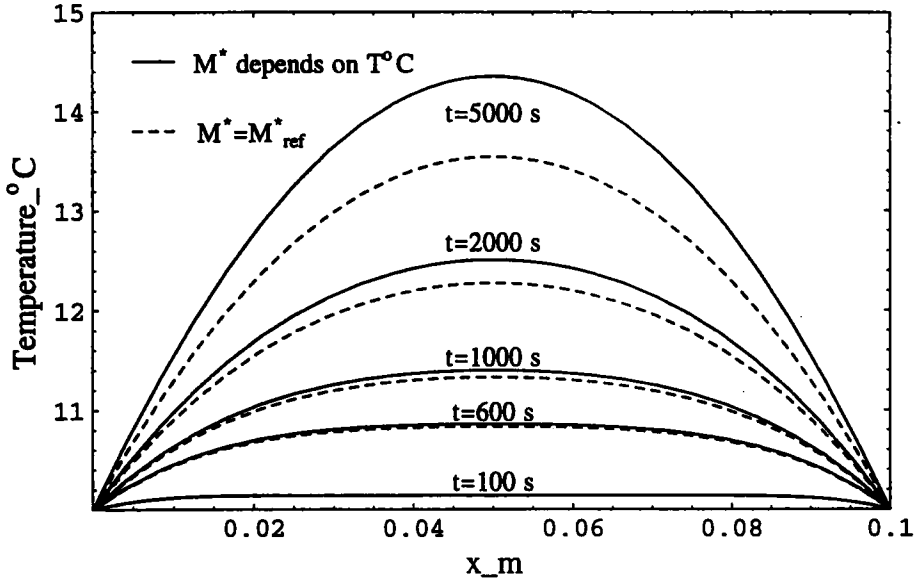

Figure 13. Temperature profiles at five different times, M^* constant or temperature-dependent.

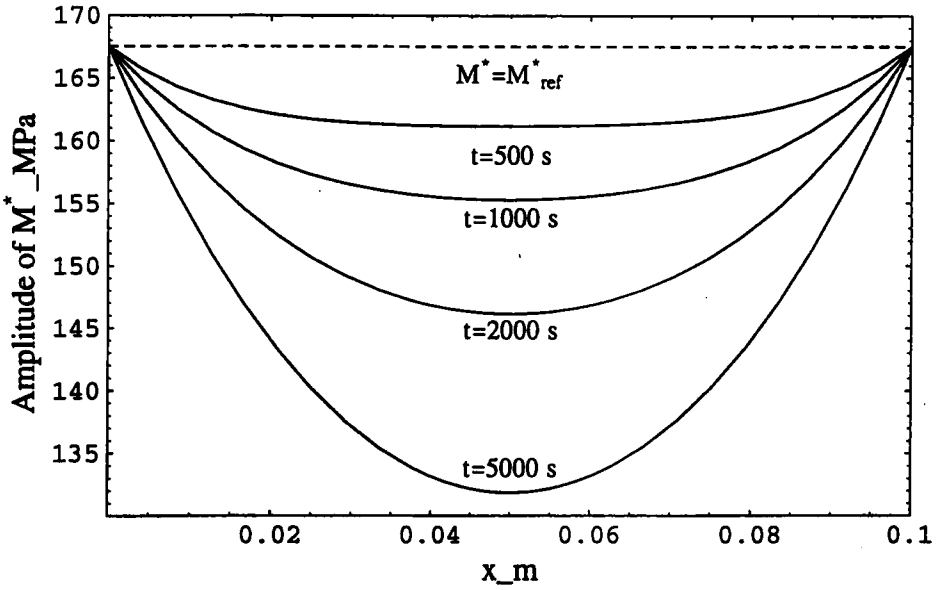

Figure 14. Profiles of the amplitude of the complex modulus $||M^*||$ at five different times.

$||e_{12}|| = \Sigma/(2||C^*||) = 1.49 \times 10^{-4}$. At 4 °C higher (for example at $t = 5000$ s in *figure 13*), the strain amplitude becomes 1.9×10^{-4} (27 % increase), in accordance with the stiffness loss.

Figure 16 plots the temperature variation in the four cases studied above: Curves A and B represents the small time variations (equivalent to adiabatical boundary conditions) extrapolated to large times, already presented in *figure 12*, while Curves C and D represent the evolution of the maximum temperature at the centre of the sample, respectively for constant and temperature-dependent modulus. Noticeably, the small time approximations

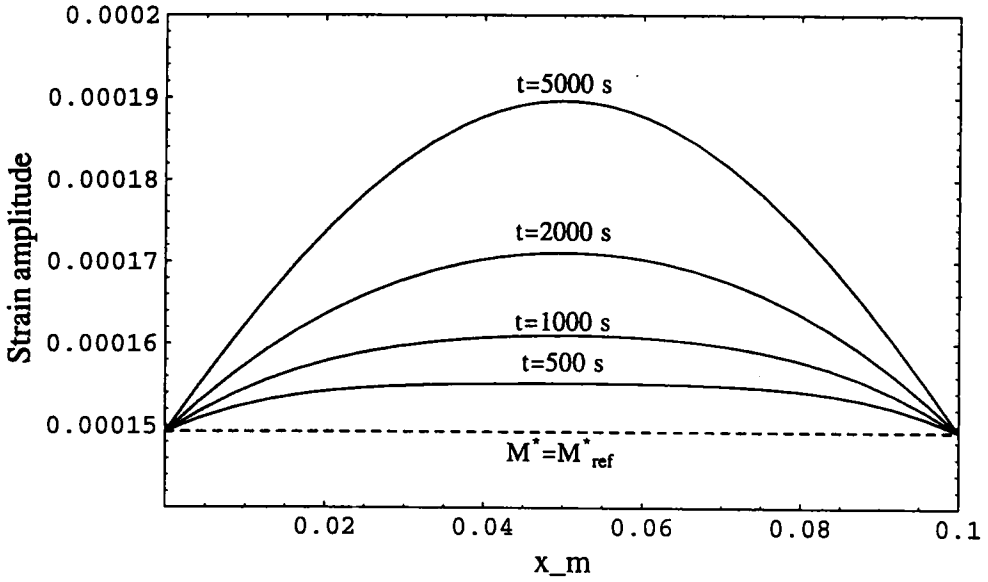

Figure 15. Profiles of the amplitude of shear strain amplitude $\gamma/2$ at five different times.

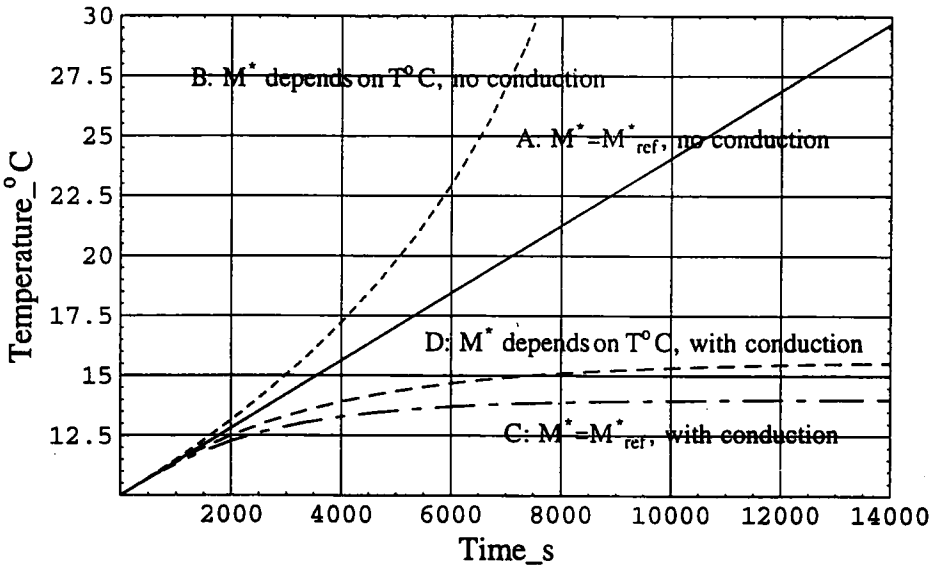

Figure 16. Temperature variations taking into account different hypotheses.

are only valid for the first 2000 s; moreover, the small temperature variations during this interval justify the assumption of constant modulus. At larger times, heat evacuated due to the boundary conditions quickly limits the temperature rises, so that a stationary state is reached somewhere between $t = 6000$ and 8000 s. Note that the characteristic time needed for the boundary conditions to reach the centre is given by $\langle \rho C \rangle L^2/\lambda_M \approx 5700$ s ($L = 5$ cm = centre to boundary distance), giving a correct 'order of magnitude' estimate of the transient duration. The case of a temperature-dependent modulus takes a longer time to reach the stationary state (around 12000 s) due to non-linear effects.

9. Conclusions

In regard to the thermal diffusion problem of a heterogeneous medium with an internal source, it has been shown by double homogenisation that four qualitatively different cases can be encountered, depending on the thermal-mechanical properties, the loading parameters (frequency, amplitude), as well as the duration of observation. For a single experiment with a set of predetermined parameters such as a bituminous concrete sample under cyclic loading, the situation evolves with time, but only part of the cases enumerated can be encountered.

The analysis of the fully coupled thermomechanical problem provides an explicit expression of the heat source term, and takes into account the time-dependent thermal-softening effect (due to the presence of a thermosensitive phase), which in the majority of cases progresses on a macrochronological time-scale. Space homogenisation reduces the computations to the case of an equivalent homogeneous medium, the 'global' behaviour being described by macroscopic variables. Time homogenisation further reduces the computations. The long-term evolutions can thus be directly computed without the need to follow the rapid temporal oscillations.

The method of analysis presented here can also be applied to other materials such as resinous concrete and more generally to heterogeneous materials containing a thermosensitive phase.

Annexe A

Asymptotic analyses of thermal conduction

The details of the asymptotic analyses leading to the results in Section 5.4 are now presented. Depending on the relative magnitudes of $t_e/\tilde{t}$ and $l/\delta_{\tilde{t}}$, supposed to be independent of each other at the present stage of analysis, the relative order of magnitude of the conductive, inertial and source terms in the heat equation will be different. The configurations considered are summarised in the following table.

Table AI. Different cases considered.

		$\varepsilon_t = \frac{t_e}{\tilde{t}}$	
		$O(1)$	$\ll 1$
$\varepsilon_l = l/\delta_{\tilde{t}}$	$O(1)$	Case i	Case ii
	$\ll 1$	Case iii	Case iv

Case i: $\varepsilon_l = O(1)$, $\varepsilon_t = O(1)$: for this case ($l/\delta_{\tilde{t}}$; $t_e/\tilde{t} = O(1)$), no macroscopic scales are possible, and the local variables y and t have to be retained

$$\mathrm{div}_y[\lambda(\nabla\theta)] = \rho C \partial_t \theta - S \tag{A1}$$

Taking into account the spatial periodicity of heat source and the microstructure and the fact that the boundary conditions only affect a thin boundary layer of $\delta_{\tilde{t}}$ at small time leaving the majority of interior points unaffected, the temperature field is Ω-periodical except over a thin boundary layer. Hence the resolution can be limited to a unit cell Ω (*figure 1*). Moreover, linearity of the problem implies that the solution can be expressed in the form of a convolution product involving a transient thermal Green's function defined on the cell.

Case ii: $\varepsilon_l = O(1)$ and $\varepsilon_t \ll 1$; this case corresponds to a long observation time compared with the excitation period, while the corresponding heat front advance remains comparable to the size of local heterogeneities.

According to Eqs (42) and (43), the heat equation can in this case be formally renormalised to take the following form, *in local coordinates* (t, y)

$$\varepsilon \mathrm{div}[\lambda(\nabla\theta)] = \rho C\dot{\theta} - \varepsilon S \tag{A2}$$

where for simplicity we have written ε for ε_t. No macroscopic length scale exists. To account for the temporal fluctuations, we seek a solution in the form of an asymptotic series

$$\theta = \theta^0 + \varepsilon\theta^1 + \varepsilon^2\theta^2 + \ldots \tag{A3}$$

where θ^i are periodical with respect to t. Zero-order terms in (A2) then lead to $\partial_t\theta^0 = 0$, in other words $\theta^0 = \theta^0(y, T)$ is independent of t. Taking into account the periodicity of θ^1, we have necessarily $\int_\tau^{\tau+t_e} \partial_t\theta^1 d\tau = 0$. Hence, first-order terms in (A2), after time averaging, give

$$\mathrm{div}_y[\lambda(\nabla_y\theta^0)] = \rho C\partial_T\theta^0 - \{S\} \tag{A4}$$

where the independent variables are y and T (ie. microscopic space description and macrochronological time description), and $\{\}$ is the temporal averaging operator

$$\{\,.\,\} = \frac{1}{t_e}\int_\tau^{\tau+t_e} (.)d\tau$$

Here again, due to the spatial periodicity and the linearity of the problem, computations can theoretically be confined to a unit cell, and the solution can once again be expressed in the form of a convolution product involving the macrochronological transient Green's function.

Case iii: $\varepsilon_t = O(1)$ and $\varepsilon_l \ll 1$; in this case, the observation time is comparable to the period while the corresponding heat front advance is very large compared to the size of local heterogeneities. This case can for example occur when heterogeneities are of extremely small size. Putting $\varepsilon = \varepsilon_1$, the equation to be solved is

$$\mathrm{div}(\lambda\nabla\theta) = \varepsilon^2\rho C\dot{\theta} - \varepsilon^2 S \tag{A5}$$

No macrochronological time-scale exists, and the time derivative $\dot{\theta}$ is simply $\partial_t\theta$, while the left-hand side $\mathrm{div}[\lambda\nabla\theta]$ admits the classic asymptotic development. Zero-order terms of (A5) lead to

$$\mathrm{div}_y(\lambda\nabla_y\theta^0) = 0 \tag{A6}$$

Hence $\theta^0 = \theta^0(x, t)$ is independent of y. The first-order terms, taking account of this result, give

$$\mathrm{div}_y[\lambda(\nabla_x\theta^0 + \nabla_y\theta^1)] = 0 \tag{A7}$$

The general solution of (A7) is, following Auriault (1983) and Francfort and Suquet (1986)

$$\theta^1(x, y, t) = \zeta(y)\nabla_x\theta^0(x, t) + \Theta^1(x, t) \tag{A8}$$

where the components $\zeta_i(y)$ are particular solutions of (A8) when $\nabla_x\theta^0$ equals the i^{th} unit vector $\underline{e}_i$. Substituting the above expression of θ^1 in the equation of second-order terms, and taking the space average, we get the following equation

$$\mathrm{div}_x[\lambda_M\nabla_x\theta^0] = \langle\rho C\rangle\partial_t\theta^0 - \langle S\rangle \tag{A9}$$

where λ_M is the macroscopic conductivity tensor, defined by

$$\lambda_M = \frac{1}{|\Omega|}\int_\Omega \lambda[I + \nabla_y\zeta(y)]d\Omega \tag{A10}$$

Here, the independent variables are x and t (i.e. macroscopic space but microchronological time description). The influence of the boundary conditions is no longer confined to the vicinity of boundary points, so that the determination of the temperature field normally requires the knowledge of the macroscopic boundary conditions.

Case iv: $\varepsilon_l \ll 1$, $\varepsilon_t \ll 1$; this corresponds to a long observation time compared to the period of excitation and a large heat front advance compared to the size of local heterogeneities. In the two previous cases, the choice of the 'small parameter' is unique and unambiguous, whereas the present case is more complicated, and a new difficulty arises on the choice of the relevant 'small parameter' in the asymptotic solution scheme. We now have to distinguish the following three subcases of interest:

$$\text{iv-a: } \frac{\varepsilon_t}{\varepsilon_1} = O(1); \quad \text{iv-b: } \frac{\varepsilon_t}{\varepsilon_1} = O(\varepsilon_1); \quad \text{iv-c: } \frac{\varepsilon_1}{\varepsilon_t} = O(\varepsilon_t)$$

Case iv-a: for $\varepsilon_t/\varepsilon_1 = O(1)$, denote $\varepsilon = \varepsilon_t = \varepsilon_1$ where the equality sign should be understood in the sense of order of magnitude. The heat equation can in this case be formally renormalised to read, *in local coordinates* (t, y)

$$\mathrm{div}[\lambda \nabla \theta] = \varepsilon \rho C \dot{\theta} - \varepsilon^2 S \tag{A11}$$

Note that this time, the double scale derivative has to be applied both to space and time derivatives. As above, we seek a solution in the form of an asymptotic series (A3). The zero-order terms in (A11) give $\mathrm{div}_y(\lambda \nabla_y \theta^0) = 0$, thus $\theta^0 = \theta^0(x, T, t)$ is independent of y.

The first-order terms give $\mathrm{div}_y[\lambda(\nabla_x \theta^0 + \nabla_y \theta^1)] = \rho C \partial_t \theta^0$, which, after taking the space average on Ω leads to $\langle \rho C \rangle \partial_t \theta^0 = 0$. Thus $\theta^0 = \theta^0(x, T)$, while the general solution of $\mathrm{div}_y[\lambda(\nabla_x \theta^0 + \nabla_y \theta^1)] = 0$ is (A8), which, taking into account the additional independent variable T, reads

$$\theta^1(x, y, T, t) = \zeta(y) \nabla_x \theta^0(x, T) + \Theta^1(x, T, t) \tag{A12}$$

The second-order terms, after taking the space average, lead to ($\partial_t \theta^1 = \partial_t \Theta^1$ independent of y)

$$\mathrm{div}_x[\lambda_M \nabla_x \theta^0] = \langle \rho C \rangle (\partial_T \theta^0 + \partial_t \theta^1) - \langle S \rangle$$

Here, only $\partial_t \theta^1$ and $\langle S \rangle$ depend on the 'local' time t, which shows that effects of source oscillations only affect terms of first-order or higher. Taking the time average of the above relation, we get the following macroscopic heat equation, depending only on the macroscopic variables x and T

$$\mathrm{div}_x[\lambda_M \nabla_x \theta^0] = \langle \rho C \rangle \frac{\partial \theta^0}{\partial T} - \langle \{S\} \rangle \tag{A13}$$

Case iv-b: for $\varepsilon_t/\varepsilon_1 = O(\varepsilon_1)$, put $\varepsilon_l = \varepsilon$ and $\varepsilon_t = \varepsilon^2$. The renormalised heat equation then reads

$$\mathrm{div}[\lambda \ \mathrm{grad}\theta] = \rho C \dot{\theta} - \varepsilon^2 S \tag{A14}$$

Note that the double-scale time derivative is now written

$$\dot{\theta} = (\partial_t + \varepsilon^2 \partial_T)[\theta^0 + \varepsilon \theta^1 + \varepsilon^2 \theta^2 + \ldots] = \partial_t \theta^0 + \varepsilon \partial_t \theta^1 + \varepsilon^2 (\partial_T \theta^0 + \partial_t \theta^2) + \ldots$$

Zero-order terms of (A14) give $\mathrm{div}_y(\lambda \nabla_y \theta^0) = \rho C \partial_t \theta^0$. Space averaging, owing to the Ω-periodicity of θ^0 then leads to $\langle \rho C \partial_t \theta^0 \rangle = 0$, independently of the value of t, whereas time averaging gives $\mathrm{div}_y(\lambda \nabla_y \{\theta^0\}) = 0$, whatever is the value of y. This is only possible if θ^0 is itself independent of y and t, in other words, $\theta^0 = \theta^0(x, T)$.

Now, first-order terms, after taking the temporal average, lead to

$$\mathrm{div}_y[\lambda(\nabla_x \theta^0 + \nabla_y \{\theta^1\})] = 0$$

giving, on account of $\theta^0 = \theta^0(x, T)$, the solution

$$\{\theta^1\}(x, y, T) = \zeta(y) \nabla_x \theta^0(x, T) + \Theta^1(x, T) \tag{A15}$$

The second-order terms then result in

$$\mathrm{div}_y[\lambda(\nabla_x\theta^1 + \nabla_y\theta^2)] + \mathrm{div}_x[\lambda(\nabla_x\theta^0 + \nabla_y\theta^1)] = \rho C[\partial_T\theta^0 + \partial_t\theta^2] - S$$

Successive spatial and temporal averaging then lead to the macroscopic description (A13) previously found.

Case iv-c: for this last case $\varepsilon_1/\varepsilon_t = O(\varepsilon_t)$, denotes $\varepsilon_t = \varepsilon$ and $\varepsilon_1 = \varepsilon^2$. The renormalised equation reads

$$\mathrm{div}[\lambda\ \mathrm{grad}\theta] = \varepsilon^3\rho C\dot{\theta} - \varepsilon^4 S \tag{A16}$$

while the conductive term, on account of the double-scale space derivative, is now written

$$\mathrm{div}(\lambda\nabla\theta) = [\mathrm{div}_y + \varepsilon^2\mathrm{div}_x][\nabla_y + \varepsilon^2\nabla_x]\{\theta^0 + \varepsilon\theta^1 + \varepsilon^2\theta^2 + \ldots\}$$

The zero- and first-order terms lead to $\theta^0 = \theta^0(x,T,t)$ and $\theta^1 = \theta^1(x,T,t)$, while the second-order terms give $\mathrm{div}_y[\lambda(\nabla_y\theta^2 + \nabla_x\theta^0)] = 0$, hence the classic solution $\theta^2 = \zeta(y)\nabla_x\theta^0 + \Theta^2(x,T,t)$. The third-order terms give $\mathrm{div}_y[\lambda(\nabla_y\theta^3 + \nabla_x\theta^1)] = \rho C\partial_t\theta^0$. Taking the space average, this leads to the conclusion that $\theta = \theta^0(x,T)$. Finally, the fourth-order terms result in

$$\mathrm{div}_y[\lambda(\nabla_y\theta^4 + \nabla_x\theta^2)] + \mathrm{div}_x[\lambda(\nabla_y\theta^2 + \nabla_x\theta^0)] = [\partial_T\theta^0 + \partial_t\theta^1] - S$$

The space–time average again leads to the completely macroscopic description (A13).

The following table summarises the space–time descriptions according to the scale factors.

Table AII. Space–time descriptions according to the scale factors.

		$\varepsilon_t = \frac{t_e}{\bar{t}}$	
		$= O(1)$	$\ll 1$
$\varepsilon_1 = l/\delta_{\bar{l}}$	$= O(1)$	Case i (y,t)	Case ii (y,T)
	$\ll 1$	Case iii (x,t)	Case iv (x,T)

References

Auriault J.L., 1983, Effective macroscopic description for heat conduction in periodic composites, Int. J. Heat Mass Transfer, 26, 6, 861–869.

Boutin C., Auriault J.L., 1990, Dynamic behaviour of porous media saturated by a viscoelastic fluid. Application to bituminous concretes, Int. J. Eng. Sci., 28, 11, 1157–1181.

Boutin C., DeLaroche C., Di Benedetto H., Ramond G., 1995, De la rhéologie du liant à celle de l'enrobé, Théorie de l'homogénéisation et validation expérimentale, Premier Séminaire Européen sur la Rhéologie — Eurobitume.

Dormieux L., Auriault J.L., Coussy O., 1993, Pore pressures generation in a seabed subjected to wave loading, Eur. J. Mech. Solids, 12, 6, 773–801.

Doubbaneh E., 1995, Comportement mécanique des enrobés bitumineux des petites aux grandes déformations, Ph.D thesis, l'INSA Lyon.

Francfort G.A., Suquet P.M., 1986, homogenization and mechanical dissipation in thermoviscoelasticity, Arch. Rat. Mech. Anal., 96, 265.

Fung Y.C., 1968, Foundations of Solid Mechanics, Prentice-Hall, New Delhi, India.

Guennouni T., 1988, Sur une méthode de calcul de structure soumise à des chargements cycliques : l'homogénéisation en temps. Math. Modell. Numer. Anal., 22, 3, 417–455.

Huet C., 1963, Étude par une méthode d'impédance du comportement des matériaux hydro-carbonés, Thèse de docteur-Ingénieur, Paris.

Piau J.M., 1989, Modélisation thermomécanique du comportement des enrobés bitumineux, Bull. Liaison Lab. Ponts et Chaussées, 163.

Sanchez-Palencia E., 1980, Non homogeneous media and vibration theory, Lecture Notes in Physics, Vol. 127, Springer-Verlag, Berlin.

Stephani C., 1981, Etude thermique des phénomènes de fatigue dans les matériaux composites bitumineux, Journées de Physiques LCPC, Les Arcs.